THEORY OF NUCLEAR MAGNETISM OF SOLID
HYDROGEN AT LOW TEMPERATURES

By

YING LIN

A DISSERTATION PRESENTED
TO THE GRADUATE SCHOOL
OF THE UNIVERSITY OF FLORIDA IN
PARTIAL FULFILLMENT OF THE REQUIREMENTS
FOR THE DEGREE OF DOCTOR OF PHILOSOPHY

UNIVERSITY OF FLORIDA

1988

ACKNOWLEDGEMENTS

TABLE OF CONTENTS

APPENDIX

Abstract of Dissertation Presented to the Graduate School
of the University of Florida in Partial Fulfillment of the
Requirements for the Degree of Doctor of Philosophy

THEORY OF NUCLEAR MAGNETISM OF SOLID
HYDROGEN AT LOW TEMPERATURES

By

Ying Lin

April 1988

Chairman: Neil Samuel Charles Sullivan
Major Department: Physics

Systematic studies of the nuclear magnetism of solid ortho-para hydrogen

mixtures at low temperatures are presented.

The formulation of the nuclear spin-lattice relaxation time T_1 for the case

of the local ordering in the orientational "glass" phase of ortho-para hydrogen

mixtures is given. The temperature dependence of T_1 is discussed. A strong

dependence on the position of the NMR isochromat in the line shape is found

and this is in good agreement with the experimental results of a group of

physicists at Duke University, provided that the cross-relaxation is taken into

account. The relaxation is found to deviate considerably from an exponential

recovery.

The orientational degrees of freedom of ortho hydrogen molecules in terms

of density matrices and the irreducible tensorial operators associated with unit

angular momentum are described. The range of allowed values for the orienta-

tional order parameters is determined from the positivity conditions imposed

on the density matrix.

A theory of solid echoes and nuclear spin stimulated echoes following a two-

pulse RF sequence and a three-pulse sequence in the quadrupolar glass phase

of solid hydrogen is developd. The stimulated echoes can be used to compare a "fingerprint" of the local molecular orientations at a given time with those at some later time (less than T_1) and thereby used to detect ultra-slow molecular re-orientations.

CHAPTER 1

INTRODUCTION

The orientational ordering of the rotational degrees of freedom of hydrogen molecules at low temperatures has been carried out by a number of groups in recent years $(1 - 19)$. The principal reason for this interest is that the ortho hydrogen (or para deuterium) molecules with unit angular momentum, $J = 1$, represent an almost ideal example of interacting "spin-1" quautum rotators, and therefore a valuable testing ground for theoretical models of co-operative behavior.

A suggestion that a random distribution of ortho molecules in a para-hydrogen matrix may behave as a quadrupolar glass at low temperatures for ortho concentration $X < 55\%$ was proposed. It was based on the observation that ortho-para hydrogen mixtures provide a striking physical realization of the combined effects of frustration and disorder on collective phenomena. These effects play a determining role in spin glasses, and the behavior of solid hydrogen mixtures is analogous to that of a spin-glass such as $Eu_xSr_{1-x}S$ in a random field(20,21).

The electrostatic quadrupole-quadrupole interaction is the dominant interaction which determines the relative orientations of the ortho molecules, and there is a fundamental topological incompatibility between the configuration for the lowest energy for a pair of molecules (a Tee Configuration for EQQ) and the crystal lattice structure: one cannot arrange all molecules so that they are mutually perpendicular on any 3D lattice.

1

At high temperatures the molecules are free to rotate, but on cooling, the ortho molecules tend to orient preferentially along local axes to minimize their anisotropic EQQ interactions. As the temperature is reduced, this leads to a continuous but relatively rapid growth of local order parameters, $(\sigma = \langle 3J_z^2 - 2 \rangle)$ which measure the degree of alignment along the local symmetry axes oz. There is a broad distribution p(σ) of local order parameters at low temperatures (12, 22, 23), but no clear phase transition has been detected (18,24).

The degree of cooperativity in the slowing down of the orientational fluctuations of the molecules as the samples are cooled is of special interest in these systems and this has motivated several independent experiemental studies(25−28) of NMR relaxation times T_1, which are determined by the fluctuations of the molecular orientations. One of the most striking results reported by S. Washburn et al. (28) is the observation of a very strong dependence of T_1 on the spectral position within the NMR absorption spectrum. While a qualitative interpretation of this behavior in terms of "sloppy" librons has been offered(1,28), a more detailed treatment has been lacking. One of the aims of my research is to extend earlier work (29) by using a straightforward theory and to compare the results with the experiemental data.

In the low concentration regime, although it is agreed that (i) the low temperature NMR lineshapes indicate a random distribution of molecular orientations (for both the local axes and and the alignment $\sigma = < 3J_z^2 - 2 >$, and (ii) that there is apparently no abrupt transition in the thermodynamic sense; there has been disagreement (1,3) over the interpretation of the behavior of the molecular orientational fluctuations on cooling from the high temperature (free rotator) phase to very low temperatures ($T < 0.1K$). While some early

work reported a very rapid, but smooth variation (25,27,30) with temperature, corresponding to a collective freezing of the orientational fluctuations, subsequent studies (14,26,28) indicated a slow, smooth dependence with no evidence of any strong collective behavior. In order to resolve this problem it is important to understand two unusual properties of the nuclear spin relaxation rates in the glass regime. These two properties which will be discussed in Chapter 3 are (i) the spectral inhomogeneity (14,29,30) of the relaxation rate T_1^{-1} across the NMR absorption spectrum, and (ii) the nonexponential decay (14,31) of the magnetization of a given isochromat; both result from the broad distribution of local axes and alignments for the molecular orientations. Both properties alone lead to variations by more than an order of magtitude and need to be understood theoretically before attempting to deduce characteristic molecular fluctuation rates from the relaxation times. It will be shown that the strong departure from exponential decay for the magnetization can be understood provided that the broad distribution of local order parameters is correctly accounted for.

In the so-called "quadrupolar glass" the quantum rotors cannot in general be described by pure states and a density matrix formalism is needed to describe the orientational degrees of freedom. It is needed to determine the precise limitations on the local order parameters (molecular alignement, etc.) from the quantum mechanical conditions imposed on the density matrix and to discuss the implications for the analysis of NMR experiments. Some of the considerations for the spin-1 density matrix description have been given elsewhere (29, 32 − 37) but solid H_2 is a special case because the orbital angular momentum is quenched. The case will be discussed in chapter 4.

In molecular solids, one has to consider two kinds of degrees of freedom: translational degrees of freedom for the centre-of-mass motion and orientational degrees of freedom for the rotational motion of the molecules.

One of the most fascinating problems encountered in the molecular solids is the existence of glass-like phases in which the molecular orientations become frozen without any significant periodic correlation from one site to another throughout the crystal. The most striking example of these "orientational glasses" is probably that observed in the solid hydrogen when the quadrupole-bearing molecules are replaced by a sufficient number of inert diluants.

If the quadrupoles in this frustrated system (20) are replaced by "inert" molecules, it leads to large reorientations of the quadrupole-bearing molecules in the neighbourhood of the inactive diluants and the dissappearance of long-range order when the quadrupole concentrations is reduced below 55%. The HCP lattice is apparently stable down to very low temperatures (7) and the NMR experiments indicate that the molecular orientations vary in a random fashion from one site to another, both the directions of the local equilibrium axes and the degree of orientation with respect to these axes vary randomly throughout a given crystal.

The important questions are (i) whether or not the freezing of the molecular motion persists for time scales much longer than those previously established for the glass phase and (ii) how the freezing occurs on cooling.

In order to answer these questions a new type of experiment was clearly needed.

The echo techniques are of great practical importance in NMR measurements on the orientationally ordered hydrogen, because they allow one to extract information which is not easily or unambiguously determinable from ei-

ther steady-state line shape or FID analyses. Conventional continuous wave (CW) and free induction decay (FID) NMR techniques have only been able to show that the orientational degrees of freedom appear to be fixed for times up to $10^{-4} - 10^{-5}$ S. A considerable improvement may be achieved by the analysis of solid echoes for which the observation times during which one can follow molecular reorientations are extended to an effective relaxation time $(T_2)_{eff}$, which may (by a suitable choice of pulses) be much longer than the transverse relaxation time T_2 that limits the conventional techniques.

It will be shown that spin echoes and stimulated echoes following a two-pulse sequence and a three-pulse sequence, respectively, provide a more powerful means of investigating the orientational states and particularly the dynamics of the molecules bearing the resonant nuclei, than the conventional continuous-wave technique.

Spin echoes were observed in solid H_2 a long time ago (38) and have been used to study the problem of orientational ordering (11, 14, 27, 28, 39, 40). In order to gain a deeper insight into this problem, a series of questions will be disscused in chapter 5. These are the formation of spin echoes (including solid echoes and stimulated echoes), explanation and comparison with experiments, and the motional damping of echoes.

CHAPTER 2

THEORY OF NMR RELAXATION

Bloembergen-Purcell-Pound Theory

The theory of spin relaxation in liquids (or gases) is based upon time-dependent perturbation theory.

In liquids where the spin-spin coupling is weak and comparable to the coupling of the spins with the lattice, it is legitimate to consider individual spins, or at most groups of spins inside a molecule, as separate systems coupled independently to a thermal bath, the lattice.

It is well known that the expression for the interaction between two magnetic dipoles of nuclear spin $\vec{I_i}$ and $\vec{I_j}$ can be expanded into 6 terms:

$$H_{DD} = \frac{\gamma_i \gamma_j \hbar^2}{r_{ij}^3} [\vec{I_i} \cdot \vec{I_j} - 3(\vec{I_i} \cdot \vec{n})(\vec{I_j} \cdot \vec{n})]$$

$$= \frac{\gamma_i \gamma_j \hbar^2}{r_{ij}^3}(A + B + C + D + E + F) \qquad (2.1)$$

where

$$A + B = \frac{1}{2}(3cos^2\theta - 1)(\vec{I_i} \cdot \vec{I_j} - 3I_{iz}I_{jz})$$

$$C = -\frac{3}{2}(I_i^+ I_{jz} + I_{iz}I_j^+)sin\theta cos\theta e^{-i\phi}$$

$$D = -\frac{3}{2}(I_i^- I_{jz} + I_{iz}I_j^-)sin\theta cos\theta e^{i\phi}$$

$$E = -\frac{3}{4}I_i^+ I_j^+ sin^2\theta e^{-2i\phi}$$

$$F = -\frac{3}{4}I_i^- I_j^- sin^2\theta e^{2i\phi}$$

6

If we carry out first-order time-dependent perturbation calculations to obtain the transition probability W between the megnetic energy levels, we find for a nuclear spin $I = \frac{1}{2}$.

$$W = \frac{3}{4}\gamma^4\hbar^2 I(I+1)[J_1(\nu_0) + \frac{1}{2}J_2(2\nu_0)] \tag{2.2}$$

and the longitudinal relaxation time

$$T_1 = \frac{1}{2W}$$

$$\frac{1}{T_1} = \frac{3}{2}\gamma^4\hbar^2 I(I+1)[J_1(\nu_0) + \frac{1}{2}J_2(2\nu_0)] \tag{2.3}$$

This is the BPP expression(41,42); where

$$J(\omega) = \int_{-\infty}^{+\infty} G(\tau)e^{i\omega\tau}d\tau$$

$$G(\tau) = \overline{F(t)F^*(t+\tau)}$$

$$F_0 = \frac{1}{r^3}(1 - 3cos^2\theta)$$

$$F_1 = \frac{1}{r^3}sin\theta cos\theta e^{i\phi}$$

$$F_2 = \frac{1}{r^3}sin^2\theta e^{2i\phi}$$

Theory for Liquids in Terms of Mori's Formalism

Daniel Kivelson and Kenneth Ogan reformulated the study of spin relaxation in liquids in terms of Mori's statistical mechanical theory of transport phenomena(43,44,45,46). They started with some well-known phenomenological magnetic relaxation relations and formulated them in a manner most suitable for comparison with Mori's theory. They obtained simple Bloch equations by the Mori method and extend the treatment to a time domain not adequately described by the Bloch equations. For this dissertation I will just demonstrate

the theory for the simple case in which the Bloch equations can describe the relaxation phenomena.

We know for a Brownian particle that the Langevin equation is a valid equation of motion for times much longer than the characteristic molecular times:

$$m\frac{d\vec{v}}{dt} = \vec{\mathcal{F}} - \varsigma\vec{v} + \vec{F}(t) \tag{2.4}$$

Where $\vec{v}$ is the velocity of the Brownian particle, $\vec{\mathcal{F}}$ is the force on it due to an externally applied field, $\varsigma\vec{v}$ represents the slow, frictional force where ς is the friction constant, and $\vec{F}(t)$ is a force which is a rapidly varying random function which averages to zero.

Mori developed a "generalized Langevin equation" which provides a division of time scales into a slow time scale associated with the motion of the Brownian particle and a fast time scale associated with collective motion.

Mori chose a set of dynamical variables, for example, $\vec{A}(t)$, which describe the relevant slow variations in the system. $\vec{A}(t)$ describes a displacement from equilibrium, i.e. $\langle\vec{A}(t)\rangle = 0$.

Let $\dot{\alpha}$ represent component of the time derivative of $\vec{A}$ that are orthogonal to $\vec{A}$, and are rapidly varying

$$\dot{\vec{\alpha}} = (1 - P)\dot{\vec{A}} \tag{2.5}$$

where P is a projection operator.

The time dependence of $\vec{A}(t)$ can be expressed in terms of the superoperator, $\mathcal{H}^x$, of the Hamiltonian as

$$\dot{\vec{A}} = i\mathcal{H}^x\vec{A} \tag{2.6}$$

$$\vec{A}(t) = e^{i\mathcal{H}^x t}\vec{A} \tag{2.7}$$

The time evolution of $\dot{\vec{\alpha}}(t_p)$ is determined by a propagator composed only of those components of the Hamiltonian $\mathcal{H}^x$, which lie outside the subspace determined by the slow variables, i.e.

$$\dot{\vec{\alpha}}(t_p) = exp[t(1-P)i\mathcal{H}^x]\dot{\vec{\alpha}} \tag{2.8}$$

We now define a memory function matrix $k(t)$, an effective memory function matrix $K(t)$ and a relaxation matrix $\hat{K}$ as follows:

Memory function matrix:

$$k(t) = \langle \dot{\vec{\alpha}}(t_P)\dot{\vec{\alpha}}\rangle \cdot \langle \vec{A}\vec{A}\rangle^{-1} \tag{2.9}$$

Effective memory function matrix:

$$K(t) = k(t)e^{-i\Omega t} \tag{2.10}$$

where

$$i\Omega = \langle \dot{\vec{A}}\vec{A}^\dagger\rangle \cdot \langle \vec{A}\vec{A}^\dagger\rangle^{-1} \tag{2.11}$$

Relaxation matrix $\hat{K}$:

$$\hat{K} = \int_0^\infty K(t)dt \tag{2.12}$$

The relaxation matrix may be complex:

$$\hat{K} = \hat{K}_{RE} - i\hat{K}_{IM} \tag{2.13}$$

The real part is associated with relaxation times and the imaginary part with frequency shifts.

Substituting (2.13) into generalized Langevin equation, we obtain the fundamental relation - Mori's equation:

$$\frac{d}{dt}\overline{\vec{A}(t)} = -[-i(\Omega + \hat{K}_{IM}) + \hat{K}_{RE}] \cdot \overline{\vec{A}(t)} \tag{2.14}$$

and its Fourier transform:

$$i\omega \vec{A}(\omega) - \vec{A}(0) = i\Omega \cdot \vec{A}(\omega) - \mathcal{K}(\omega - \Omega) \cdot \vec{A}(\omega) \qquad (2.15)$$

We can now derive Bloch's equation and relaxation time formulae in a simple case (one variable).

We express the Hamiltonian as

$$\mathcal{H} = \mathcal{H}_S + \mathcal{H}_L + \mathcal{H}_{SL} \qquad (2.16)$$

where $\mathcal{H}_S$ depends only on the spin variable, $\mathcal{H}_L$ represents the molecular motions and interactions which are independent of the spins, and $\mathcal{H}_{SL}$ involves those interactions which involve both spins and nuclear spatial coordinates.

The slow variables $\vec{A}$ can be selected as:

$$\vec{A} = \begin{pmatrix} S_+ \\ \Delta S_z \\ S_- \end{pmatrix} \qquad (2.17)$$

We assume that $k(t)$, the memory function matrix, decays rapidly so that $\mathcal{K}(\omega - \Omega)$ can be replaced by $\mathcal{K}_{RE} - i\mathcal{K}_{IM}$. Equation (2.15), transformed back to the time domain, then becomes:

$$\frac{d}{dt}\overline{S_z(t)} = -T_1^{-1}[\overline{S_z(t)} - \langle S_z \rangle] \qquad (2.18)$$

$$\frac{d}{dt}\overline{S_\pm(t)} = [i(\pm\omega_0 + \sigma_\pm) - T_2^{-1}]\overline{S_\pm(t)} \qquad (2.19)$$

where

$$T_1^{-1} = Re\hat{K}_{zz} = \frac{4}{N}\int_0^\infty \langle [\mathcal{H}_{SL}(t_p), S_z(t_p)][S_z, \mathcal{H}_{SL}]\rangle \, dt \qquad (2.20)$$

$$T_2^{-1} = (\hat{K}_{RE})_{\pm\pm}$$

$$= Re(\frac{2}{N})\int_0^\infty \langle [\mathcal{H}_{SL}(t_p), S_\pm(t_p)][S_\mp, \mathcal{H}_{SL}]\rangle e^{\mp i\omega_0 t} \, dt \qquad (2.21)$$

$$\sigma_\pm = (\hat{K}_{IM})_{\pm\pm} = Im(\frac{2}{N})\int_0^\infty \langle [\mathcal{H}_{SL}(t_p), S_\pm(t_p)][S_\mp, \mathcal{H}_{SL}]\rangle e^{\mp i\omega_0 t} \, dt \qquad (2.22)$$

Equations (2.18) and (2.19) are the simple Bloch equations except that the $\sigma_\pm$ term which represents the so-called nonsecular or dynamic frequency shift is given explicitly.

Kubo and Tomita Theory

The theory originally introduced by Kubo and Tomita emphasizes the similarity of magnetic relaxation to other non-equlibrium phenomena (46,47,48,49).

Description

We know that the Bloch equation can describe the relaxation of the magnetization $\vec{m}$. It is a linear equation.

$$\frac{d\vec{m}}{dt} = \gamma \vec{m}(t) \times \vec{H}(t) - \frac{m_x(t)\vec{i} + m_y(t)\vec{j}}{T_2} - \frac{m_z(t) - m_z^0}{T_1}\vec{k} \qquad (2.23)$$

In matrix notation the Bloch equation (2.23) can be written as

$$\Delta \dot{\vec{m}}(t) = -L \cdot \Delta \vec{m}(t) \qquad (2.24)$$

where

$$\Delta m_k(t) = m_k(t) - m_k^0 \quad (k = i, j, k) \qquad (2.25)$$

m_k^0 is the thermal equilibrium value

$$-L = \begin{pmatrix} -\frac{1}{T_1} & 0 & 0 \\ 0 & -\frac{1}{T_2} - i\omega_0 & 0 \\ 0 & 0 & -\frac{1}{T_2} + i\omega_0 \end{pmatrix} \qquad (2.26)$$

If we transform from the laboratory frame to a frame rotating with the Larmor frequency around the z axis, we will have

$$\Delta \dot{\vec{m}}(t) = -L' \Delta \vec{m}^R(t) \qquad (2.27)$$

The formal solution of Eq. (2.24) is the following:

$$\Delta m_\alpha(t) = (e^{-Lt})_{\alpha\beta} \Delta m_\beta(t) \qquad (2.28)$$

The Fourier transform of the formal solution is therefore

$$\Delta \hat{m}_\alpha(\omega)_+ = (\frac{1}{L - i\omega})_{\alpha\beta} \Delta m_\beta(0) \qquad (2.29)$$

+ means a positive Fourier transform and in the rotating frame:

$$\Delta m_j(\omega)_+ = (\frac{1}{L'_{jj} - i\omega})\Delta m_j(0) \tag{2.30}$$

<u>Response Function</u>

The linear response formalism begins by calculating the linear response of a dynamic variable to a disturbance created by a time-dependent external force.

Consider the Hamiltonian:

$$H_{total}(t) = H - \varsigma M_l H_l(t) \tag{2.31}$$

where

(i) H describes all the interactions responsible for the motions of the spins, including the effect of the large, static Zeeman field.

(ii) $H_l(t)$ is a small, time-varying field which is responsible for the nonequlibrium behavior of the system.

The response function $f_{kl}(t)$ is defined as

$$\Delta m_k(t) = \int_{-\infty}^{t} f_{kl}(t - \tau)H_l(\tau)d\tau \tag{2.32}$$

The response function $f_{kl}(t)$ gives the effect of the disturbance at time t. The Fourier transform of eq. (2.32) is

$$\Delta m_k(\omega) = \chi_{kl}(\omega)H_l(\omega) \tag{2.33}$$

where

$$\chi_{kl}(\omega) = \int_{0}^{\infty} e^{i\omega t}f_{kl}(t)dt \tag{2.34}$$

Equation (2.34) defines the susceptibility $\chi_{kl}(\omega)$. It has a real and imaginary part that are connceted by the Kramers-Kronig relations. The imaginary part

of the susceptibility is called the absorptive part which is related to the power the sample absorbs. The real part of the susceptibility is called the dispersive part and is related to the measured line shape.

Relaxation Function

The relationship between the relaxation function $F_{kl}(t)$ and the response function $f_{kl}(t)$ is given by

$$F_{kl}(t) = \int_t^\infty f_{kl}(\tau)d\tau \tag{2.35}$$

The relaxation function describes the time change of the response after the external disturbance is cut down to zero.

Assume a step disturbance:

$$H_l(t) = H_l e^{\epsilon t}\theta(t) \tag{2.36}$$

where

$$\theta(t) = \begin{cases} 1 & t \leq 0 \\ 0 & t > 0 \end{cases} \tag{2.37}$$

and ϵ is a small positive constant that will be taken to zero at the end of the calculation. In principle this disturbance corresponds to having a field in addition to the Zeeman field.

The response to the step disturbance in the limit $\epsilon \to 0$ is:

$$\Delta m_k(t) = F_{kl}(t)H_l \quad t > 0 \tag{2.38}$$

and

$$\Delta m_k(0) = F_{kl}(0)H_l \tag{2.39}$$

Here $F_{kl}(t)$ is the relaxation function which describes how the response to a step function disturbance decays in time.

If we regard equations (2.38) and (2.39) as matrix equations and formally eliminate the external force in these two equations, we obtain

$$\Delta m_\alpha(t) = F_{\alpha\gamma}(t) F_{\gamma\beta}^{-1}(0) \Delta m_\beta(0) \quad t > 0 \tag{2.40}$$

The central assumption of the linear response theory is that Eqs. (2.40) and (2.28) can be combined to yield a molecular expression for L as

$$[e^{-Lt}]_{\alpha\beta} = F_{\alpha\gamma}(t) F_{\gamma\beta}^{-1}(0) \tag{2.41}$$

We define $\sigma_{kl}(\omega)$ as the following

$$\sigma_{kl}(\omega) = \frac{\chi_{kl}(\omega) - \chi_{kl}(0)}{i\omega} = \int_0^\infty dt\, e^{i\omega t} F_{kl}(t) \tag{2.42}$$

From equations (2.38) and (2.39):

$$\Delta m_\alpha(\omega) = \sigma_{\alpha\beta}(\omega) H_\beta \tag{2.43}$$

$$\Delta m_\alpha(0) = \chi_{\alpha\beta}(0) H_\beta \tag{2.44}$$

$$\Delta m_\alpha(\omega) = \sigma_{\alpha\gamma}(\omega) \chi_{\gamma\beta}^{-1}(0) \Delta m_\beta(0) \tag{2.45}$$

Comparing equation (2.28) with equation (2.45) yields

$$\left(\frac{1}{L - i\omega}\right)_{\alpha\beta} = \sigma_{\alpha\gamma}(\omega) \chi_{\gamma\beta}^{-1}(0) = \frac{\sigma_{\alpha\gamma}(\omega)}{\chi_{\gamma\beta}(0)} \tag{2.46}$$

in the rotating frame

$$\frac{1}{L'_{kk} - i\omega} = \frac{\sigma_{k-k}(\omega + K\omega_0)}{\chi_{k-k}(0)} \quad k = 0, \pm 1 \tag{2.47}$$

i.e.

$$\frac{L'_{kk}}{L'^2_{kk} + \omega^2} = \frac{Re\sigma_{k-k}(\omega + K\omega_0)}{\chi_{k-k}(0)} \tag{2.48}$$

Using a symmetric form of σ_{k-k}, equation (2.48) becomes

$$\frac{L'_{kk}}{L'^2_{kk} + \omega^2} = \frac{Re\sigma_{k-k}(\omega)}{\chi_{k-k}(0)} \tag{2.49}$$

Time correlation Function Formulas for Transport Coefficients

The transport coefficient is expressed as a time integral of a correlation function of magnetization. These formulas will be derived in the limit of weak coupling between the spin and lattice degrees of freedom.

We assume that the Hamiltonian of the system $H(\lambda)$ can be split into two parts: a part H_0 that contains the Zeeman Hamiltonian and a part H' that couples the spins to the lattice and is responsible for the relaxation:

$$H(\lambda) = H_0 + \lambda H' \tag{2.50}$$

We also assume the transport coefficient $L'(\lambda)$ may be developed in a power series in λ with a leading term in λ^2:

$$L'(\lambda) = \lambda^2 \sum_n \lambda^n L'(n) \tag{2.51}$$

Since we are assuming weak coupling, we identify the measured transport coefficient with the first term of the sum in Eq. (2.45), i.e. $\lambda^2 L'(0) = L'(\lambda)$. The results of transport coefficients are

$$L_{00} = \frac{1}{T_1} = \frac{(\frac{i}{\hbar})^2}{2\langle \Delta M_z^2 \rangle} \int_0^\infty dt \langle [H', M_z][H'(t), M_z] \rangle_0 + C.C. \tag{2.52}$$

$$L_{11} = L_{-1-1} = \frac{1}{T_2}$$

$$= \frac{(\frac{i}{\hbar})^2}{4\chi T_2} \int_0^\infty dt \{ \langle [H', M_+][H'(t), M_-] \rangle_0$$

$$+ \langle [H'(t), M_-][H', M_+] \rangle_0 + C.C. \} \tag{2.53}$$

where

$$\chi T_2 = \frac{1}{2} \langle [\Delta M_-, \Delta M_+]_+ \rangle_0 \tag{2.54}$$

$$H'(t) = e^{\frac{i}{\hbar} H_0 t} H' e^{-\frac{i}{\hbar} H_0(t)} \tag{2.55}$$

The subscript zero on the braket indicates that the trace is taken over the equilibrium density matrix

$$\rho_0 = \frac{exp(-\beta H_0)}{Tr(exp(-\beta H_0))} \qquad (2.56)$$

which does not involve the spin-lattice coupling.

Nuclear Spin-Lattice Relaxation in Non-Metallic Solids

The problem here is essentially the same as that for liquids and gases, namely to calculate the probability of a flip of a nuclear spin caused by its coupling with the thermal motion of a "lattice." There are, however, some significant differences. The internal motion in solids will often have much smaller amplitudes and/or much longer correlation times than in liquids. In rigid solids because of the tight coupling between nuclear spins exemplified by frequent flip-flops between neighbours, the correct approach to nuclear magnetism is a collective one, where single large spin-system with many degrees of freedom are to be considered, rather than a collection of individual spins. The assumption is usually made that the strong coupling of the nuclei simply establishes a common temperature called a "spin temperature," and that the lattice coupling causes this temperature to change(50,51,52).

A quite general equation can be derived.

$$\frac{d\beta}{dt} = -\frac{1}{T_1}(\beta - \beta_0) \qquad (2.57)$$

where

$\beta = \frac{1}{KT_s}$ T_s - Spin temperature

$\beta_0 = \frac{1}{KT}$ T - Temperature of the lattice

Under certain conditions (practically all experimental situations), high spin and lattice temperature, Abragam and Slichter (51,52) give the following result

$$\frac{1}{T_1} = \frac{1}{2}\frac{\sum_{n,m} W_{mn}(E_n - E_m)^2}{\langle \mathcal{H}_0^2 \rangle} \tag{2.58}$$

Where $| m \rangle$ and $| n \rangle$ are the eigenstates of $\mathcal{H}_0$.

$W_{mn} = W_{nm}$ is the transition probability from the state $| m \rangle$ to the state $| n \rangle$.

There is another way to calculate T_1. It is a density matrix method, which is quite general and especially suited to discussing cases in which motional narrowing takes place. Let the density matrix ρ describe the behavior of the combined quantum mechanical system, spins + lattice. In the interaction representation

$$\rho^* = e^{-\frac{i}{\hbar}\mathcal{H}_0 t}\rho e^{\frac{i}{\hbar}\mathcal{H}_0 t} \tag{2.59}$$

$$\frac{\hbar}{i}\frac{d\rho^*}{dt} = -[\mathcal{H}_1^*(t), \rho^*] \tag{2.60}$$

Where $\mathcal{H}_1$ is a perturbation,

$$\mathcal{H}_1^*(t) = e^{-\frac{i}{\hbar}\mathcal{H}_0 t}\mathcal{H}_1 e^{\frac{i}{\hbar}\mathcal{H}_0 t}$$

Equation(2.60), integrated by successive approximation, gives

$$\frac{d\rho^*}{dt} = -\frac{i}{\hbar}[\mathcal{H}_1^*(t), \rho^*(0)] - \frac{1}{\hbar^2}\int_0^t dt'[\mathcal{H}_1^*(t), [\mathcal{H}_1^*(t'), \rho^*(0)]]$$

$$+higher\,order\,terms \tag{2.61}$$

or

$$\frac{d\rho^*}{dt} = -\frac{i}{\hbar}[\mathcal{H}_1^*(t), \rho^*(0)] - \frac{1}{\hbar^2}\int_0^t d\tau[\mathcal{H}_1^*(t), [\mathcal{H}_1^*(t-\tau), \rho^*(0)]]$$

$$+higher\,order\,terms \tag{2.62}$$

Since all the observations are performed on the spin system, all the relevant information is contained in the reduced density matrix σ^*

$$\sigma^* = tr_f\{\rho^*\} \tag{2.63}$$

with matrix elements $(\alpha \mid \sigma^* \mid \alpha') = \sum_f (f\alpha \mid \rho^* \mid f\alpha')$.

By making some assumptions Abragam (51) gives a general master equation

$$\frac{d\sigma^*}{dt} = -\int_0^\infty \overline{[\mathcal{H}_1^*(t),[\mathcal{H}_1^*(t-\tau),\sigma^*-\sigma_0]]}d\tau \tag{2.64}$$

where the bar represents an average of many particles.

If there is a spin temperature, then

$$\mathcal{H}_0\frac{d\beta}{dt} = \frac{1}{2}(\beta_0-\beta)\int_{-\infty}^{+\infty}\overline{[\mathcal{H}_1^*(t),[\mathcal{H}_1^*(t-\tau),\mathcal{H}_0]]}d\tau \tag{2.65}$$

i.e.

$$\frac{d\beta}{dt} = -\frac{1}{2}\frac{(\beta_0-\beta)}{\langle\mathcal{H}_0^2\rangle}\int_{-\infty}^{+\infty}\overline{\langle[\mathcal{H}_1^*(t),\mathcal{H}_0][\mathcal{H}_1^*(t-\tau),\mathcal{H}_0]\rangle}d\tau \tag{2.66}$$

$$\frac{1}{T_1} = \frac{1}{2}\frac{1}{\langle\mathcal{H}_0^2\rangle}\int_{-\infty}^{+\infty}\overline{\langle[\mathcal{H}_1^*(t),\mathcal{H}_0][\mathcal{H}_1^*(t-\tau),\mathcal{H}_0]\rangle}d\tau \tag{2.67}$$

For the relaxation of like spins by dipolar coupling the result for T_1 is the same as the result of Kubo and Tomita theory.

Nuclear Spin-Lattice Relaxation for Solid Hydrogen

The molecular hydrogens $(H_2,D_2,HD,\text{etc.})$ form the simplest molecular solids. The properties of solid mixtures of ortho (angular momentum $J = 1$, nuclear spin $I = 1$) and para $(J = 0, I = 0)$ hydrogen molecules have been extensively studied both theoretically and experimentally in the past decade (53,54,55,56). A popular method of experimentally probing this system has been through nuclear magnetic relaxation studies (57,58,59,60). The relaxation is determined by the orientational fluctuations of the molecules which

is in turn determined by the EQQ interaction between the ortho molecules. This relaxation rate, which is a consequence of the intramolecular nuclear spin interactions, is given by (56,61)

$$\frac{1}{T_1} = \frac{16}{3}\pi^3\{c^2 J_1^1(\omega_0) + d^2[\frac{9}{5}J_2^1(\omega_0) + \frac{16}{5}J_2^2(2\omega_0)]\} \qquad (2.68)$$

Where c denotes the constant of spin-rotational coupling and d that of the intramolecular dipolar coupling, with respective values of 113.9 and 57.7 khz. The spectral density functions $J(m\omega)$ are taken at ω_0 and $2\omega_0$ where ω_0 is the Larmor frequency(51,p278).

We consider two regimes.

The High Concentration Regime

A. B. Harris (56) calculated the spectral functions for the correlation functions for both infinite and finite temperatures. He used a high temperature expansion method to calculate the second moment and obtained good agreement with the high concentration experiments of Amstutz et al. (62), with regard to both the temperature and concentration dependence of the relaxation time.

Myles and Ebner (63) used a high temperature diagrammatic technique, combined with a simlple method of impurity averaging over the distribution of O-H_2 molecules. The averaged equations were then solved numerically to obtain the spectral functions for solid H_2 self-consistently for the first time. The resulting spectral functions were used to compute the T_1 as a function of the ortho-molecule concentration and this was shown to agree well with experiments at 10K and over concentraiton range of $0.5 \leq X \leq 1$. They obtained a $\sqrt{X}$ concentration dependence for T_1, which was in agreement with the data of Amstutz and colleagues (62) for $X > 0.5$.

The Low Concentration Regime

The low concentration regime $(X < 0.5)$ had been explored by Sung(64), A.B. Harris(56), Hama et al. (65),Ebner and Sung (66), and Ebner and Myles (67) at an earlier date. Recently, the work has been concentrated on $X < 0.5$ and very low temperatures $(T < 400mk)$, which details we will discuss in Chapter 3.

Sung (64) applied the high temperature statistical theory, developed for paramagnetic resonance with a small concentration of spins, to the calculation of the angular momemetum correlation functions and Harris used an improved version of the same theory. The T_1 resulting from these calculations had a concentration dependence of $X^{\frac{5}{3}}$, which was in agreement with the data of Weinhaus and Meyer (61), but the magnitude of T_1 obtained in this way was in disagreement with that data.

Hama et al. (65) developed a theory which was capable of treating the $T = \infty$ correlation functions at all concentrations and which gave a concentration dependence and magnitude for T_1 which were in fair agreement with experiment for all X (61,62).

Both methods had the defect that the impurity averaged correlation functions were obtained by statistically averaging assumed functional forms and no attempt was made to determine the shape of the spectral function.

The first attempt in the small X region to calculate the high temperature correlation functions self-consistently and thus to overcome the above defect was made by Ebner and Sung (66). They used the Sung and Arnold (68) method of impurity averaging the Blume and Hubbard (69) correlation function theory and obtained a T_1 which had the experimentally observed $X^{\frac{5}{3}}$

concentration dependence at small X. Since they made no attempt to properly account for the anisotropy of the intermolecular interactions, they did not obtain quantitative agreement with the experimental magnitude of T_1.

Ebner and Myles (67) improved the calculation of Ebner and Sung by properly treating the anisotropy of the electric quadrupole-quadrupole (EQQ) interaction, which is the dominant orientationally dependent interaction between two $O - H_2$ molecules in solid H_2 and which therefore, almost totally determined the shape of the angular momentum spectral functions.

Sung and Arnold's method of impurity averaging the infinite temperature Blume and Hubbard (69) correlation function equations was employed, but the equations were obtained using the full EQQ interaction rather than an isotropic approximation to it. The spin-lattice relaxation time was computed as a function of the $O - H_2$ concentration using a formula for $\frac{1}{T_1}$ derived by applying the Blume and Hubbard theory (69) to the nuclear spin correlation functions in this system. The resulting T_1 was compared to the data of Weinhaus et al. (61) at a temperature of $T = 10K$ and agreement was generally good with regard to both its magnitude and concentration dependence.

CHAPTER 3

NUCLEAR SPIN LATTICE RELAXATION

Formulation of Longitudinal Relaxation Time T_1

There is a striking resemblance between the phase diagram for the magnetic

alloys such as CuMn, AuFe ... and orientationally ordered ortho-hydrogen-

para-hydrogen alloys(Fig.1-2).

The nuclear spin-lattice relaxation of ortho molecules at low temperatures

is determined by the modulation of the intramolecular nuclear dipole-dipole

interactions H_{DD} and the spin-rotational coupling H_{SR} by the fluctuations of

the molecular orientations(55, 56). The calculations are particularly transpar-

ent if we use orthonormal irreducible tensorial operators O_{2m} and N_{2m} for the

orientational $(J = 1)$ and nuclear spin $(I = 1)$ degrees of freedom, respectively.

The O_{2M} are given by

$$O_{20} = \frac{(3J_z^2 - 2)}{\sqrt{6}}$$

$$O_{2\pm 1} = \mp \frac{1}{2}(J_\pm J_z + J_z J_\pm)$$

$$O_{2\pm 2} = \frac{1}{2}(J_\pm)^2 \tag{3.1}$$

and similar expressions hold for the N_{2m} in the manifold $I = 1$.

The intramolecular nuclear dipole-dipole interaction H_{DD} and the spin-

rotation interaction H_{SR} can be written in the above notation as

$$H_{DD} = hD \sum_i N_{2m}^\dagger(i) O_{2m}(i)$$

22

and

$$H_{SR} = -hC \sum_i (-1)^m N_{1m}^\dagger(i) O_{1m}(i) \tag{3.2}$$

respectively. D=173.1 khz and C=113.9 khz. The index i labels the ith molecule. The O_{lm} and N_{lm} are the operator equivalents of the spherical harmonics Y_{lm} in the manifolds $J = 1$ and $I = 1$, respectively.

The relaxation rate due to H_{DD} can be shown to be

$$T_{1DD}^{-1} = \frac{1}{\langle I_z^2 \rangle} \int_0^\infty \langle [I_z, \mathcal{H}_{DD}] \, [\mathcal{H}_{DD}^*(t), I_z] \rangle_T dt$$

$$= \frac{1}{\langle I_z^2 \rangle} \int_0^\infty \langle [I_z, \mathcal{H}_{DD}] \, [e^{\frac{i}{\hbar}H_0 t} \mathcal{H}_{DD} e^{-\frac{i}{\hbar}H_0 t}, I_z] \rangle dt \tag{3.3}$$

where $H_o = \hbar \omega_o I_z$. It is the Hamiltonian responsible for the molecular dynamics. Using the commutators $[I_z, N_{2m}] = m N_{2m}$ we find

$$T_{1DD}^{-1} = \frac{1}{2} D^2 \sum_{|m|=1,2} m^2 J_{2m}(m\omega_0) \tag{3.4}$$

where the spectral density at the Larmor frequency

$$J_{2m}(\omega_0) = \int_{-\infty}^\infty \langle O_{2m}(t) O_{2m}^\dagger(0) \rangle_T e^{-i\omega_0 t} dt \tag{3.5}$$

The expectation value $< ... >_T$ must be calculated with respect to the fixed Z axis given by the direction of the external magnetic field. This is the quantization axis for the nuclear Zeeman Hamiltonian, which is perturbed by the weaker H_{DD} and H_{SR} terms. The orientational order parameters, however, are evaluated with respect to the local molecular symmetry axes. We must therefore consider the rotations

$$O_{2m} = \sum_\mu d_{m\mu}^{(2)}(\chi) O_{2\mu} \tag{3.6}$$

where the $d_{m\mu}$ are the rotation matrix elements for polar angles $\chi = (\alpha, \beta)$ defining the orientation of OZ in the local (x,y,z) reference frame.
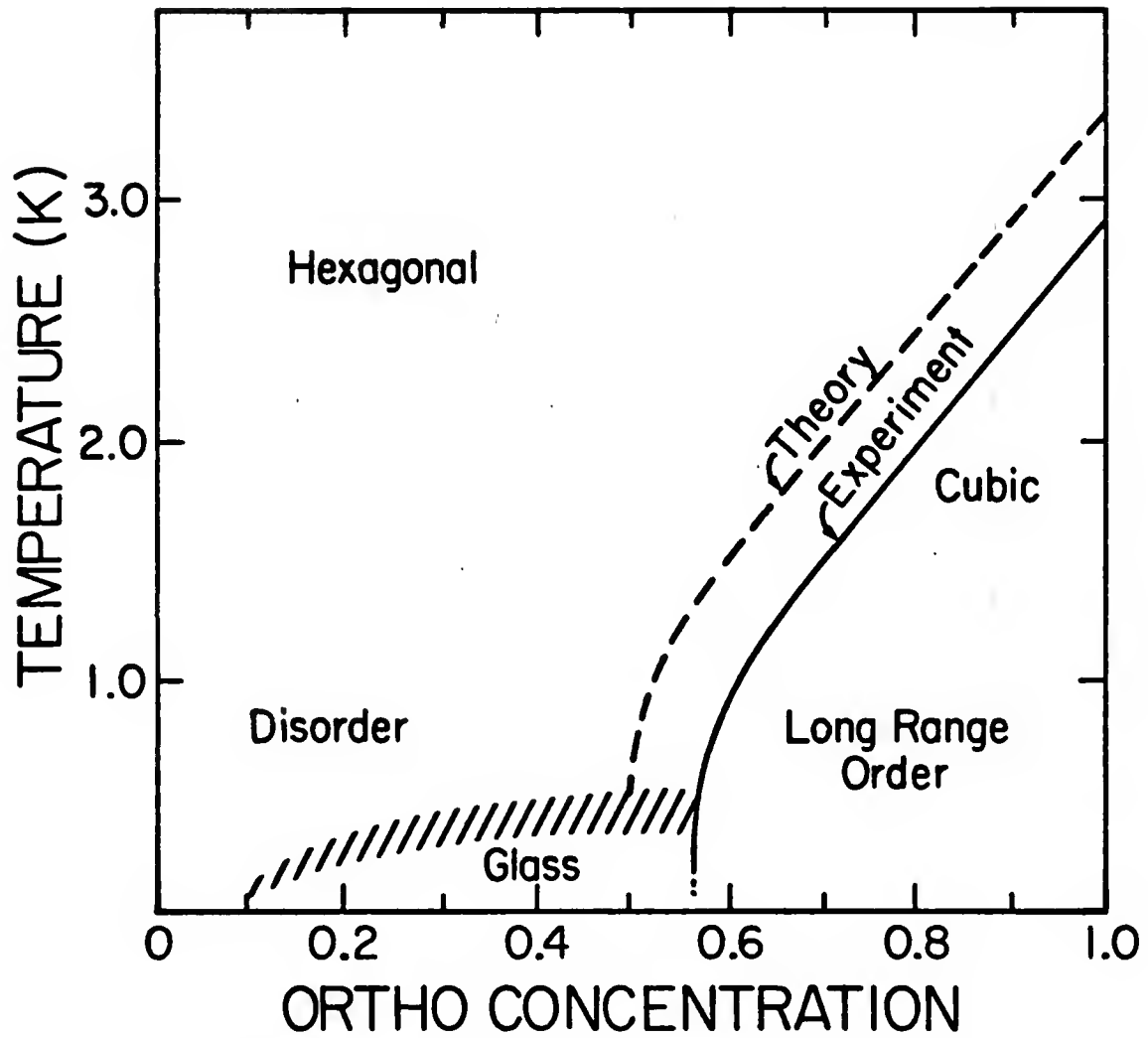
Figure 1. Phase Diagram of Ortho-Para H_2 Mixtures
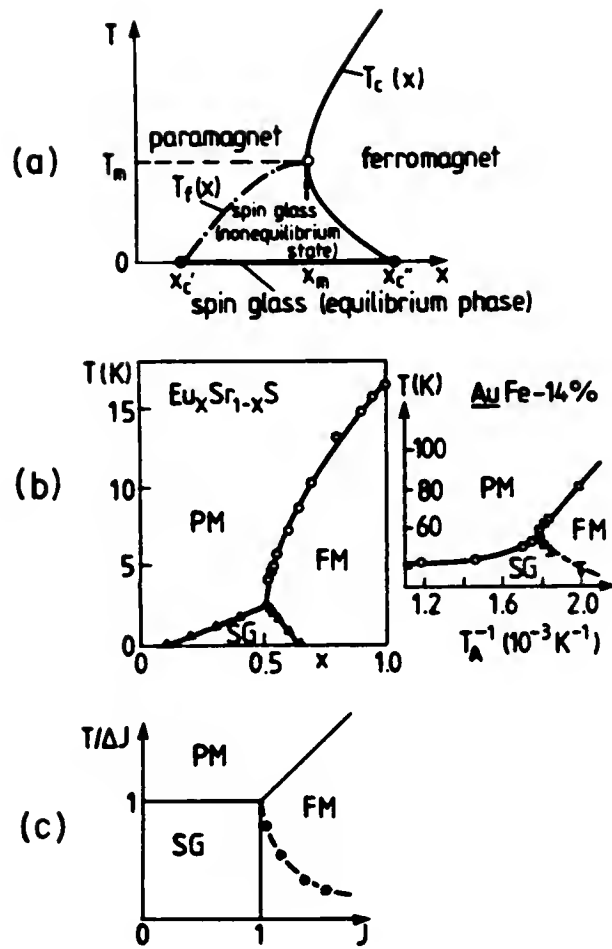
Figure 2. (a) Theoretical Phase
Diagram for A Short Range System
(b) Experimental Phase Diagram for
$Eu_xSr_{1-x}S$ And AuFe (c) Phase
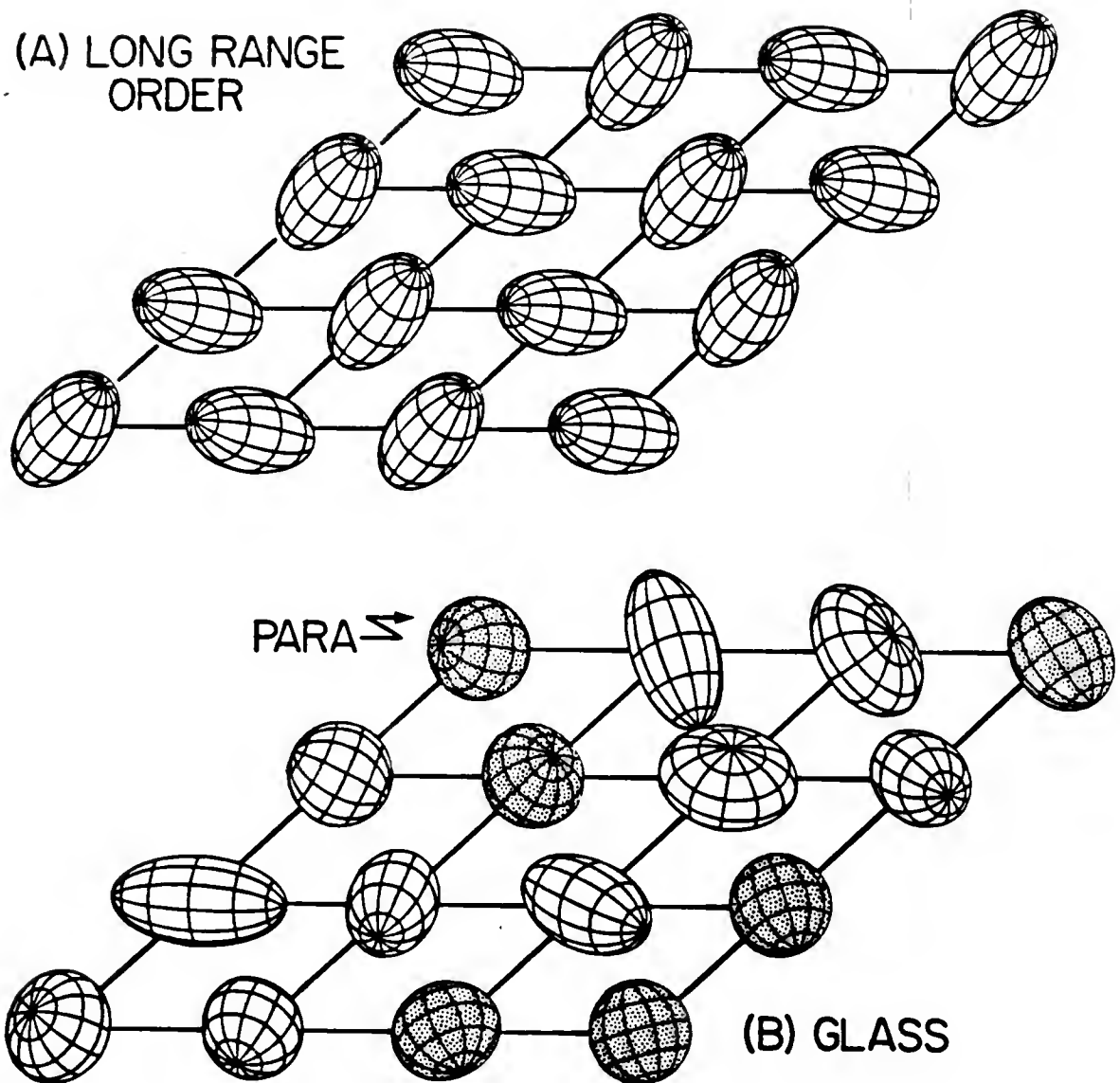Diagram of The Ising Spin Glass

Figure 3. Picture of Long Range
Order And Quadrupolar Glass

We assume the simplest possible case

$$\langle O_{2m}(t)O_{2m}^{\dagger}(0)\rangle = \langle O_{2m}(0)O_{2m}^{\dagger}(0)\rangle g_{2m}(t) \tag{3.7}$$

In the following, we consider only this case and further assume that the relaxation is dominated by the fluctuations of the $\mu = 0$ component. We find

$$T_{1DD}^{-1} = \frac{1}{12}(2 - \sigma - \sigma^2)D^2 \sum_{m=1,2} m^2|d_{m0}(\alpha)|^2 g_{20}(m\omega_0) \tag{3.8}$$

where the $g_{20}(m\omega_0)$ are the Fourier transforms of the reduced correlation functions $g_{20}(t)$ and $\sigma = \langle 3J_z^2 - 2\rangle_T$. The prefactor $(2 - \sigma - \sigma^2)$ is the mean square deviation of the operator O_{20} evaluated in the local symmetry axis frame.

The contribution from the spin-rotational interaction H_{SR} is

$$T_{1SR}^{-1} = \frac{1}{2}C^2 J_{11}(\omega_0) = \frac{1}{6}C^2(2 + \sigma)|d_{10}(\alpha)|^2 g_{10}(\omega_0) \tag{3.9}$$

the total rate $T_1^{-1} = T_{1DD}^{-1} + T_{1SR}^{-1}$

Temperature Dependence of T_1

Minimum Values of T_1

From the previous result (3.8 and 3.9)

$$\frac{1}{T_1}(\sigma, \theta) = \frac{1}{T_{1DD}}(\sigma, \theta) + \frac{1}{T_{1SR}}(\sigma, \theta)$$

where

$$\frac{1}{T_{1DD}}(\sigma, \theta) = \frac{1}{12}(2 - \sigma - \sigma^2)D^2 \sum_{m=1,2} m^2|d_{m0}(\theta)|^2 g_{20}(m\omega_0)$$

$$\frac{1}{T_{1SR}}(\sigma, \theta) = \frac{1}{6}C^2(2 + \sigma)|d_{10}(\theta)|^2 g_{10}(\omega_0)$$

If we take a powder sample average, the T_{1SR} is small.

$$\frac{1}{T_{1DD}}(\sigma) = \frac{1}{12}(2 - \sigma - \sigma^2)D^2 \left[\frac{1}{5}g_{20}(\omega_0) + \frac{4}{5}g_{20}(2\omega_0)\right] \tag{3.10}$$

To a good approximation we have

$$\frac{1}{T_1}(\sigma) \approx \frac{1}{12}(2 - \sigma - \sigma^2)D^2 \left[\frac{1}{5}g_{20}(\omega_0) + \frac{4}{5}g_{20}(2\omega_0)\right] \qquad (3.11)$$

For the simplest case we can restrict σ to negative values with appropriate definitions of principal axes (22 and Chapter 4)

$$\frac{\bar{1}}{T_1} = \frac{\int_{-2}^{0}(2 - \sigma - \sigma^2)d\sigma}{\int_{-2}^{0} d\sigma} \times \frac{1}{12}D^2 \left[\frac{1}{5}g_{20}(\omega_0) + \frac{4}{5}g_{20}(2\omega_0)\right]$$

$$= \frac{1}{36}D^2(g_{20}(\omega_0) + 4g_{20}(2\omega_0)) \qquad (3.12)$$

Assume $g_{20}(\omega_o)$ and $g_{20}(2\omega_o)$ can be taken to be in the Lorentzian form:

$$g_{20}(\omega_0) = \frac{\tau_c}{1 + \omega_0^2 \tau_c^2} \qquad (3.13)$$

$$g_{20}(2\omega_0) = \frac{\tau_c}{1 + 4\omega_0^2 \tau_c^2} \qquad (3.14)$$

when $\omega_0 \tau_c \approx 0.6156$, $T_1 = T_{1min}$

The eqs. $(3.12) - (3.14)$ result in the following

1)

$\omega_0 = 2\pi \times 100 \times 10^6$

$T_{1min} = 13.4172\,msec$

2)

$\omega_0 = 2\pi \times 25 \times 10^6$

$T_{1min} = 3.3542\,msec$
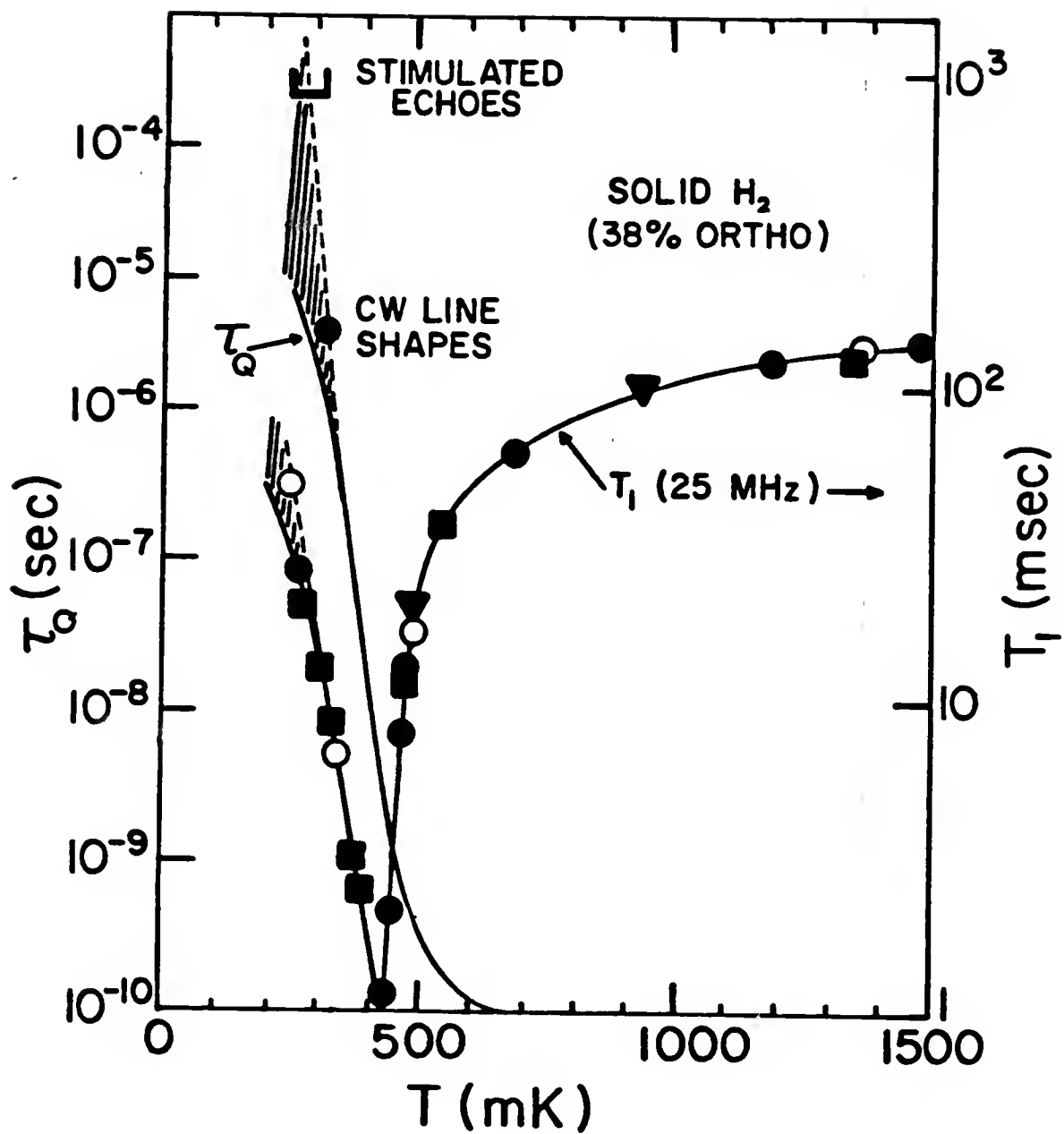
$T_{1exp} = 1.03\,msec - Fig.4$ (ref.25)

3)

$\omega_o = 2\pi \times 9 \times 10^6$

$T_{1min} = 1.20574\,msec$

$T_{1exp} = 2.25\,msec - Fig.5$ (ref.70)

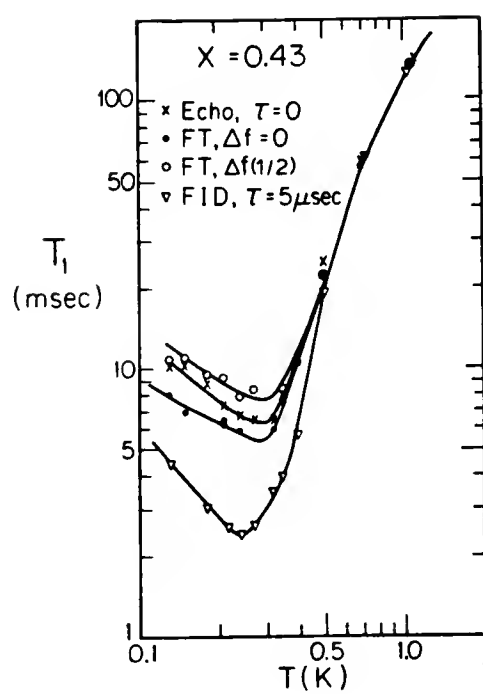Figure 4. Experimental Curve of T_1

Figure 5. Experimental Curve of T_1

Temperature Dependence of T_1

It has been observed that for the solid, a Gaussian Free Induction Decay is a good approximation for small t and so we should also consider a Gaussian form for $g_{20}(m\omega_0)$ for high frequencies. From eqs. (3.7) and (3.8):

$$\langle O_{2m}(0)O_{2m}^{\dagger}(0)\rangle g(t) = \langle O_{2m}(0)O_{2m}^{\dagger}(0)\rangle e^{-\frac{t^2}{a^2}} \tag{3.15}$$

$$g(\omega) = \int_{-\infty}^{\infty} e^{-\frac{t^2}{a^2}} e^{-i\omega t} dt = a\sqrt{\pi} e^{-\frac{\omega^2 a^2}{4}} \tag{3.16}$$

Eq. (3.12) becomes

$$\frac{1}{T_1} = \frac{D^2\sqrt{\pi}}{36}(ae^{-\frac{\omega_0^2 a^2}{4}} + 4ae^{-\omega_0^2 a^2}) \tag{3.17}$$

$$T_1 = \frac{36}{D^2\sqrt{\pi}} \frac{1}{ae^{-\frac{\omega_0^2 a^2}{4}} + 4ae^{-\omega_0^2 a^2}} \tag{3.18}$$

T_1 passes through a minimum when $\frac{dT_1}{da} = 0$, i.e for $a = 5.082 \times 10^{-9}$, and the minimum value is $T_{1min} = 1.1384 msec$, at $\frac{\omega_0}{2\pi} = 25 MHz$. The result of the theoretical value $T_{1min} = 1.1384msec$ is in very good agreement with the experimental value $T_{1min} = 1.03\,msec(25)$.

Now the question is how T_1 varies at fixed ω_0 over a wide range of temperatures which causes τ_c to vary. Similar to the discussion of the dynamics of spin glasses (71), we would like to try an Activation Law of the Vogel-Fulcher type:

$$a = a_o e^{-\left(\frac{A}{T-T_0}\right)} \tag{3.19}$$

where

A is the activation energy in temperature unit

a_0 is a time factor which is the value of a as $T \rightarrow \infty$, and

T_0 is some characteristic temperature (transition temperature), such that as $T \rightarrow T_0$, long relaxation times become important.
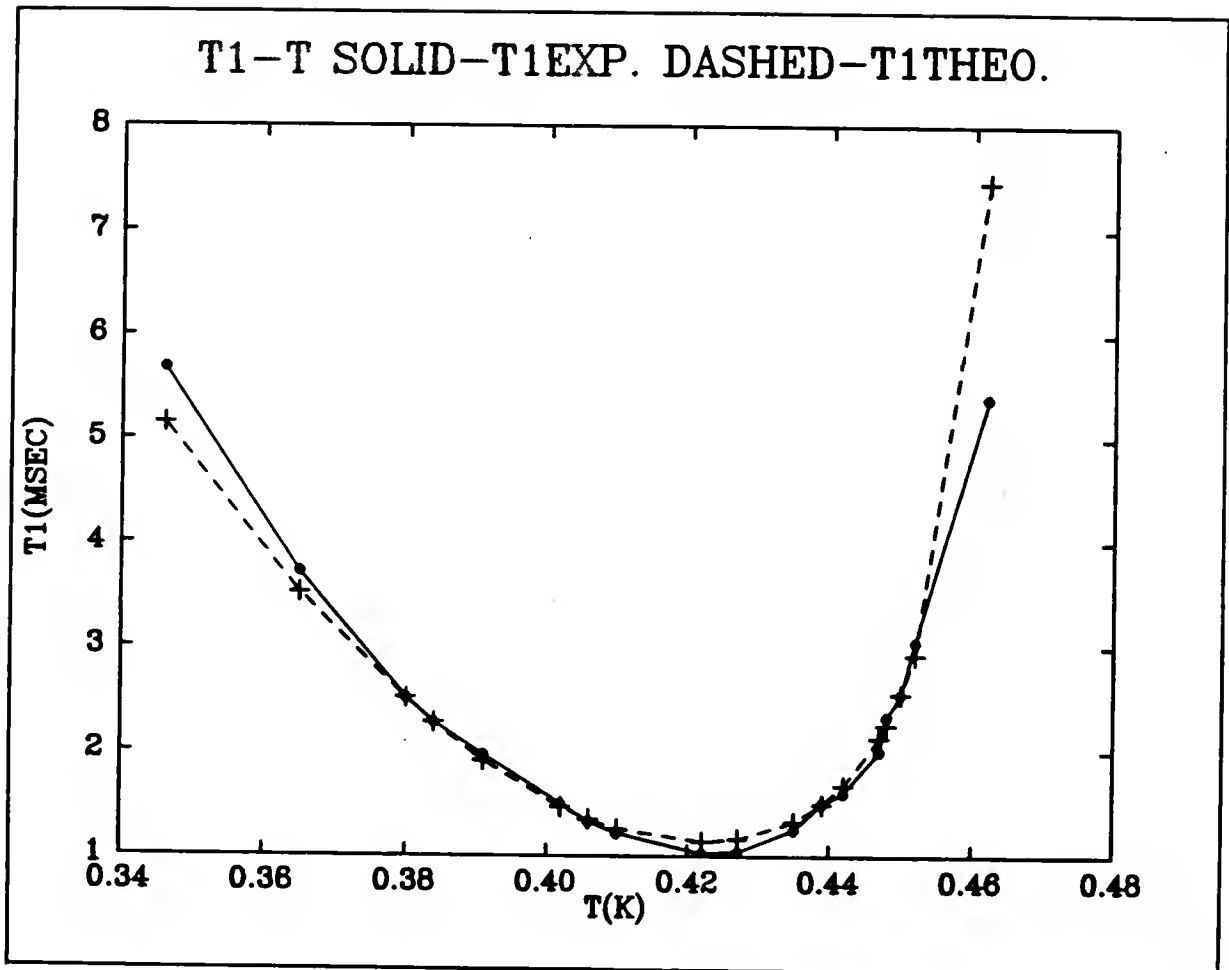
Figure 6. T_1-T Curve (solid-T_{1exp},dashed-T_{1theo})

By using two experimental values ($T_1 = 2.550 msec$ at $T = 0.450K$ and $T_1 = 2.514 msec$ at $T = 0.380K$ for $X = 38\%$) we find the following formula:

$$a = 5.4128 \times 10^{-8} \times e^{\frac{0.1880}{T - 0.5015}} \tag{3.20}$$

The Fig.6 shows curves of results of calculation and experiment. The solid line is experimental curve(25) and the dashed line is theoretical curve.

Spectral Inhomogeneity of T_1

Results of Calculations

The dependence of T_1 on $\Delta\nu$ was evaluated by considering the line shape to be a sum of Pake doublets. Each Pake doublet consists of a positive branch given by $\Delta\nu = +\frac{1}{2}DP_2(\alpha)\sigma$ and a negative branch given by $\Delta\nu = -\frac{1}{2}DP_2(\alpha)\sigma$ (Fig.7). As previously demonstrated we restrict σ to negative values. That is

$$\Delta\nu = -D\frac{|\sigma|}{2}\frac{1}{2}(3cos^2\alpha - 1) \; (positive\, branch)$$

$$\Delta\nu = D\frac{|\sigma|}{2}\frac{1}{2}(3cos^2\alpha - 1) \; (negative\, branch)$$

In order to test the theory against the experimental data we consider only the low temperature limit for which the fluctuations are slow compared to the Larmor frequency ω_0. In this case the spectral density functions are given by $g(\omega_0) = 4g(2\omega_0) \doteq \frac{1}{\omega_0^2\tau}$ (low temperature limit of Lorentz form), where τ^{-1} is the characteristic fluctuation rate, which was taken to be a unique value for simplifying calculations.

For the dipolar contribution at fixed σ and $\Delta\nu$ we obtain

$$T_{1DD}^{-1} = \frac{\frac{1}{24}(2 - \sigma - \sigma^2)D^2\left[1 - (\frac{2\Delta\nu}{D\sigma})^2\right]}{\omega_0^2\tau} \tag{3.21}$$
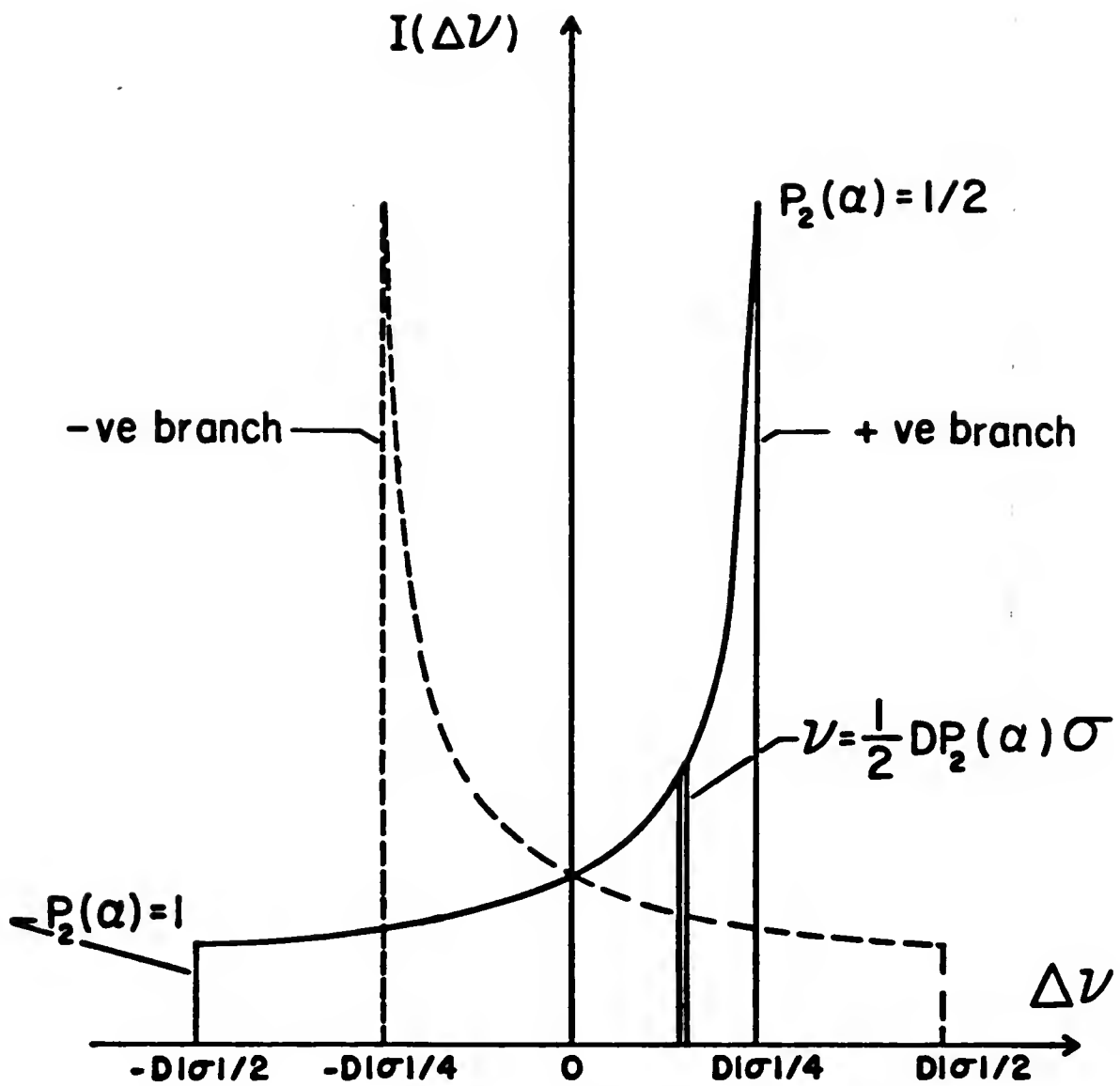
Figure 7. Allowed Range of Values of σ for
A Given Frequency $\Delta\nu$

and for the spin-rotational contribution:

$$T_{1SR}^{-1} = \frac{\frac{1}{18}C^2(2-|\sigma|)(1\pm\frac{2\Delta\nu}{D|\sigma|})}{\omega_0^2\tau} \tag{3.22}$$

The frequency dependence should be obtained by summing over all allowed σ for a given frequency $\Delta\nu$. The calculations were straightforward but quite tedious. Table I and Table II show the numerical results.

Table I Spectral Dependence of Dipole-Dipole Relaxation Rate T_{1DD}^{-1}

Frequency range $\Delta\nu$	$T_{1DD}^{-1} \times (\frac{24\omega_0^2\tau}{D^2})$	
$0 \le \Delta\nu \le \frac{1}{2}D$	$\frac{10D^2-12\nu D+4\nu^2}{3D^2} + \frac{2\nu^2}{D(D-2\nu)}\log\frac{2\nu}{D} + \frac{2\nu^2}{D(D-\nu)}\log\frac{\nu}{D}$	
$\frac{1}{2}D \le \Delta\nu \le D$	$\frac{5D^2-7\nu D+8\nu^2}{3D^2} + \frac{2\nu^2}{D(D-\nu)}\log\frac{\nu}{D}$	

Table II Spectral Dependence of Spin-Rotational Relaxation Rate T_{1SR}^{-1}

Frequency range $\Delta\nu$	$T_{1SR}^{-1} \times (\frac{18\omega_0^2\tau}{C^2})$	
$0 \le \Delta\nu \le \frac{1}{2}D$	$\frac{2D-3\nu}{D} - \frac{2\nu}{D-2\nu}\log\frac{2\nu}{D} + \frac{2\nu}{D-\nu}\log\frac{\nu}{D}$	
$\frac{1}{2}D \le \Delta\nu \le D$	$\frac{D+\nu}{D} + \frac{2\nu}{D-\nu}\log\frac{\nu}{D}$	

Discussion

Fig.8 shows the results of the calculations for the dipolar contribution T_{1DD}^{-1} and the spin-rotational contribution T_{1SR}^{-1} as function of frequency. All curves in this figure have been normalized to unity at $\Delta\nu = 0$ in order to facilitate the comparison with the experimental data. The net relaxation rate $T_{1(calc)}^{-1} = T_{1DD}^{-1} + T_{1SR}^{-1}$. The curves show discontinuities in slope at $|\Delta\nu| = \frac{D}{2}$, but this was not seen experimentally. If we take the finite cross-relaxation rate T_{12}^{-1} into

account, which will bring the very slowly relaxing isochromats at $|\Delta\nu| = 2D$ into communication with the rapidly relaxing components,

$$T_1^{-1} = T_{1(calc)}^{-1} + T_{12}^{-1} \qquad (3.23)$$

when the individual spin-lattice relaxation times are much longer than the cross-relaxation times the spins come to a common spin temperature via the cross-relaxation mechanism before relaxing to the lattice via the rapidly relaxing components. On the other hand, when the direct spin-lattice relaxation is fast and $T_1 \ll T_{12}$, the magnetization of each molecule relaxes directly to the lattice and the spins do not achieve a common spin temperature. In this latter case the nuclear magnetization will be spatially inhomogeneous.

Yu et al. (14) defined T_{12} by the probability of a spin flip-flop transition via the intermolecular dipole-dipole interaction for two isochromats ν_1 and ν_2 given by

$$
\begin{aligned}
T_{12}^{-1} &= (T_2^{flip-flop})^{-1} exp \left[-\frac{\pi^2(\nu_1 - \nu_2)^2}{M_2^{inter}} \right] \\
&= (T_2^{flip-flop})^{-1} exp \left[-\frac{M_2^{intra} - (M_1^{intra})^2}{2M_2^{inter}} \right] \qquad (3.24)
\end{aligned}
$$

where the exponential factor is the overlap given by Abragam (51) for two lines centred at ν_1 and ν_2 and their individual widths are determined by the intermolecular dipole-dipole interaction. M_2^{intra}, M_1^{intra} and M_2^{inter} are the moments resulting from the intra- and inter-molecular dipole-dipole interactions, respectively. Yu et al. (14) observed a much weaker dependence than the exponential variation with M_2^{intra} given by the overlap factor. Due to the discrepancy between theory and experiment we chose the empirical values reported by Yu et al. (14) as the most reliable estimate of T_{12}.
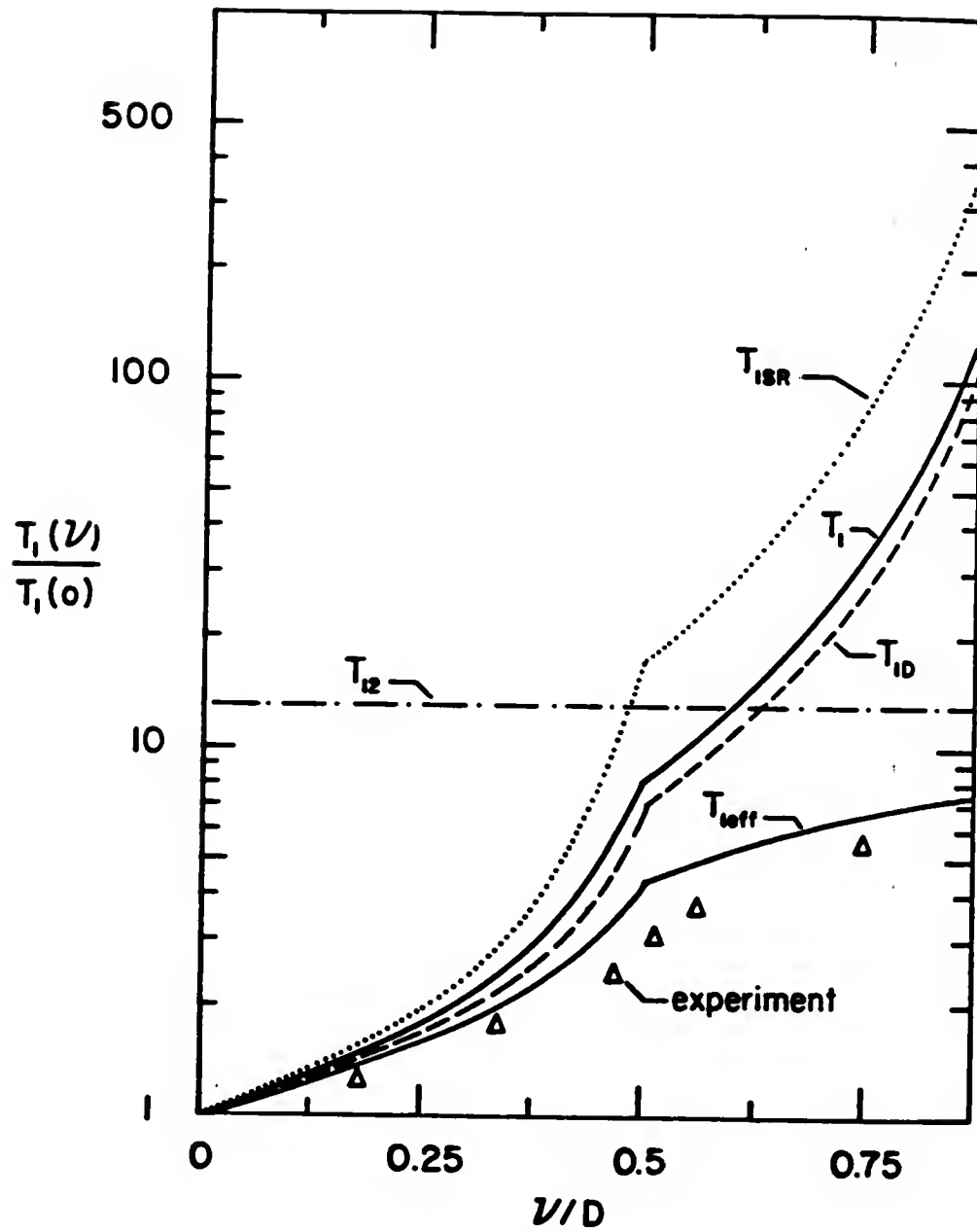
Figure 8. Frequency Dependence of T_1

The most complete studies of the spectral inhomogeneity of T_1 in the quadrupolar glass phase has been carried out for an ortho concentration $X = 0.45$ at $T = 0.15K(14)$, and the data of ref.14 would place the cross-relaxation time T_{12} in the range $7.5 - 10.5$ msec.

While the cross-relaxation is faster than the direct relaxation to the lattice, the values of T_{12} reduce the spectral inhomogeneity of the relaxation of the NMR line shape. In this case we expect to observe $T_{1(obs)}^{-1} = T_{1(cal)}^{-1} + T_{12}^{-1}$ for the relaxation of the magnetization of a given isochromat. This is shown in Fig.8. In view of the uncertainties in the cross-relaxation and the simplifying assumptions that have been made, the overall agreement with the experimental results is good. The correct overall behavior is predicted as well as the subtle change in spectral dependence at the half width points which has already been seen in the experimental data of Yu et al. (14).

Non-Exponential Relaxation of Nuclear Magnetization

Although it is agreed that (i) the low temperature NMR lineshapes indicate a random distribution of molecular orientations (for both the local axes and the alignment $\sigma = \langle 3J_z^2 - 2 \rangle$), and (ii) that there is apparently no abrupt transition in the thermodynamic sense; there has been disagreement (1,3) over the interpretation of the behavior of the molecular orientational fluctuations on cooling from the high temperature (free rotator) phase to very low temperatures $(T < 0.1K)$. Is it a very rapid, but smooth variation (25,27,70) with temperature, corresponding to a collective freezing of the orientational fluctuations or a slow, smooth dependence (9,14,28) with no evidence of any strong collective behavior? In order to resolve this problem it is important

to understand two unusual properties–the spectral inhomogeneity of the relaxation rate T_1^{-1} across the NMR absorption spectrum (14,29,30,72) and the non-exponential decay of the magnetization of a given isochromat (14). The spectral inhomogeneity has been discussed previously and the purpose of this part is to show that the strong departure from exponential decay for the magnetization can be understood provided that the broad distribution of local order parameters is correctly accounted for.

<u>Variation of Relaxation Rates within Given Isochromats</u>

As previously proved (3.21,3.22)

$$T_{1DD}^{-1} = \frac{\frac{1}{24}(2 - \sigma - \sigma^2)D^2 \left[1 - (\frac{2\Delta\nu}{D\sigma})^2\right]}{\omega_0^2\tau}$$

$$T_{1SR}^{-1} = \frac{\frac{1}{18}(2 - |\sigma|)C^2(1 \pm \frac{2\Delta\nu}{D|\sigma|})}{\omega_0^2\tau}$$

The frequency of a particular component of the NMR absorption line is given by

$$\Delta\nu = \pm\frac{1}{2}DP_2(\alpha)\sigma \qquad (3.25)$$

and this can be satisfied by very different values of σ and α; e.g. $\Delta\nu = \frac{1}{4}D$ occurs for $\sigma = -1, P_2 = \frac{1}{2}$; $\sigma = -\frac{1}{2}, P_2 = 1; \sigma = -\frac{2}{3}$, $P_2 = \frac{3}{4}$....; the only constraints being that σ and P_2 lie within their limits; $-2 \leq \sigma \leq 0$, and $-\frac{1}{2} \leq P_2 \leq 1$. Obviously, different pairs of σ and P_2 (for fixed $\Delta\nu$) can result in very different values of T_{1DD} and T_{1SR}. Molecules which contribute to the same isochromat of the NMR line but which have different values of σ and P_2 will therefore relax at different rates. This is illustrated in table III,IV and V, which give the variation of T_1 for $\Delta\nu = \frac{1}{2}D$, $\frac{1}{4}D$ and 0, respectively. The relative contribution of these rates can be determined from the probabilities

$\Pi(\sigma),\Pi(P_2)$ of finding σ and P_2. At low temperatures, the analysis of the line-shape indicates that a good approximation for $\Pi(\sigma)$ is a triangular distribution $\Pi(\sigma) \propto \sigma$ (12,23). For P_2 we assume a powder distribution of local axes (i.e. very glassy) which requires that $\Pi(P_2) \propto \dfrac{1}{\sqrt{\frac{(2P_2+1)}{3}}}$. The calculated rates $T_1^{-1}(\sigma, P_2)$ have a relative weight $P = \Pi(\sigma) \times \Pi(P_2)$ for the relaxation of the component $\Delta\nu = \mp\frac{1}{2}D|\sigma|P_2$.

Magnetization ratio

$$\frac{M(t)}{M(0)} = \frac{\sum Pe^{-\frac{t}{T_1}}}{\sum P} \tag{3.26}$$

The weighted relaxations using the indicated probabilities are given in Fig.9 and Fig.10. The experimental results reported by Yu et al. (14) for different $\Delta\nu$ are indicated by the symbols.

Table III Variation of Relaxation Rates within A Given Isochromat $(\Delta\nu = \frac{1}{2}D)$

parame. $P_2(\alpha)$	parame. $|\sigma|$	prob. $\Pi(P_2)$	prob. $\Pi(\sigma)$	rates T_{1SR}^{-1}	rates T_{1DD}^{-1}	rates[a] T_1^{-1}	
$\frac{15}{16}$	$\frac{16}{15}$	1.022	1.067	0.058	0.234	0.267	
$\frac{7}{8}$	$\frac{8}{7}$	1.044	1.143	0.107	0.431	0.492	
$\frac{13}{16}$	$\frac{16}{13}$	1.069	1.231	0.144	0.583	0.666	
$\frac{3}{4}$	$\frac{4}{3}$	1.095	1.333	0.167	0.681	0.777	
$\frac{11}{16}$	$\frac{16}{17}$	1.124	1.455	0.170	0.706	0.804	
$\frac{5}{8}$	$\frac{8}{5}$	1.155	1.600	0.150	0.634	0.720	
$\frac{9}{16}$	$\frac{16}{9}$	1.188	1.778	0.097	0.422	0.478	
$\frac{1}{2}$	2	1.225	2.000	0.0	0.0	0.0	

[a]Rates given in units of $\dfrac{D^2}{24\omega_0^2\tau}$

The Determination of The Molecular Correlation Time τ and T_1 at $\Delta\nu = 0$

The only unknown parameter for eqs. (3.21) and (3.22) is the molecular correlation time τ and the best fit represented by the solid lines and the broken

Table IV Variation of Relaxation Rates within A Given Isochromat ($\Delta\nu = \frac{1}{4}D$)

parame. $P_2(\alpha)$	parame. $|\sigma|$	prob. $\Pi(P_2)$	prob. $\Pi(\sigma)$	rates T_{1SR}^{-1}	rates T_{1DD}^{-1}	rates[a] T_1^{-1}	
$\frac{15}{16}$	$\frac{8}{15}$	1.022	0.533	0.092	0.272	0.325	
$\frac{7}{8}$	$\frac{4}{7}$	1.044	0.571	0.179	0.526	0.629	
$\frac{13}{16}$	$\frac{8}{13}$	1.069	0.615	0.260	0.760	0.910	
$\frac{3}{4}$	$\frac{2}{3}$	1.095	0.667	0.333	0.972	1.165	
$\frac{11}{16}$	$\frac{8}{11}$	1.119	0.727	0.398	1.159	1.389	
$\frac{5}{8}$	$\frac{4}{5}$	1.155	0.800	0.450	1.316	1.576	
$\frac{9}{16}$	$\frac{8}{9}$	1.188	0.889	0.486	1.435	1.715	
$\frac{1}{2}$	1	1.225	1.000	0.500	1.500	1.789	
$\frac{7}{16}$	$\frac{8}{7}$	1.265	1.143	0.482	1.485	1.763	
$\frac{3}{8}$	$\frac{4}{3}$	1.309	1.333	0.417	1.337	1.577	
$\frac{5}{16}$	$\frac{8}{5}$	1.359	1.600	0.275	0.938	1.097	
$\frac{1}{4}$	2	1.414	2.000	0.0	0.0	0.0	

[a]Rates given in units of $\frac{D^2}{24\omega_0^2\tau}$

line at $\Delta\nu = 0$ in Fig.9, is obtained $\tau = 1.51 \times 10^{-7}S$. For

$$\tau = 1.51 \times 10^{-7}S$$

$$\frac{1}{T_1}\mid_{\Delta\nu=0} = 1.49597 \times \frac{10^3}{10.0446}$$

$$T_1\mid_{\Delta\nu=0} = 6.7144(msec) \qquad (3.27)$$

T_1 at $\Delta\nu = 0$ is 6.71 ms which is in excellent agreement with the experimental value of $6.6 \pm 0.5ms$ (14,70).

Since D=173.1 khz, in Fig.9 the $\Delta\nu$ for the calculated $\frac{M(t)}{M(o)}$ are 87,43.5 and 0 khz which are below the values chosen by the Duke group (14). The same theroy to calculate $\frac{M(t)}{M(0)}$ for $\Delta\nu = 98$ and 58 khz and the results are depicted in Fig.10. The overall agreement is very satisfactory.

Comparison of the calculated decays $M_{\Delta\nu}(t)$ with the experimental results shows that not only is the correct overall deviation from exponential decay

predicted, but that there is also a significant long tail to the decay which ought to be tested for experimentally. This long time behavior is unique to the glassy regime of the hydrogen mixtures.

Table V Variation of Relaxation Rates within A Given Isochromat ($\Delta\nu = 0$)

parame. $|\sigma|$	prob. $\Pi(\sigma)$	rates T_{1SR}^{-1}	rates T_{1DD}^{-1}	rates[a] T_1^{-1}	
$\frac{8}{15}$	0.533	1.467	2.249	3.096	
$\frac{4}{7}$	0.571	1.429	2.245	3.070	
$\frac{8}{13}$	0.615	1.385	2.237	3.036	
$\frac{2}{3}$	0.667	1.333	2.222	2.992	
$\frac{8}{11}$	0.727	1.273	2.198	2.933	
$\frac{4}{5}$	0.800	1.200	2.160	2.853	
$\frac{8}{9}$	0.889	1.111	2.099	2.740	
1	1.000	1.000	2.000	2.577	
$\frac{8}{7}$	1.143	0.857	1.837	2.331	
$\frac{4}{3}$	1.333	0.667	1.556	1.940	
$\frac{8}{5}$	1.600	0.400	1.040	1.271	
2	2.000	0.0	0.0	0.0	

We consider $P_2(\alpha) = 0$ for the range of $|\sigma|$ considered in Table IV in order to facilitate the comparison.
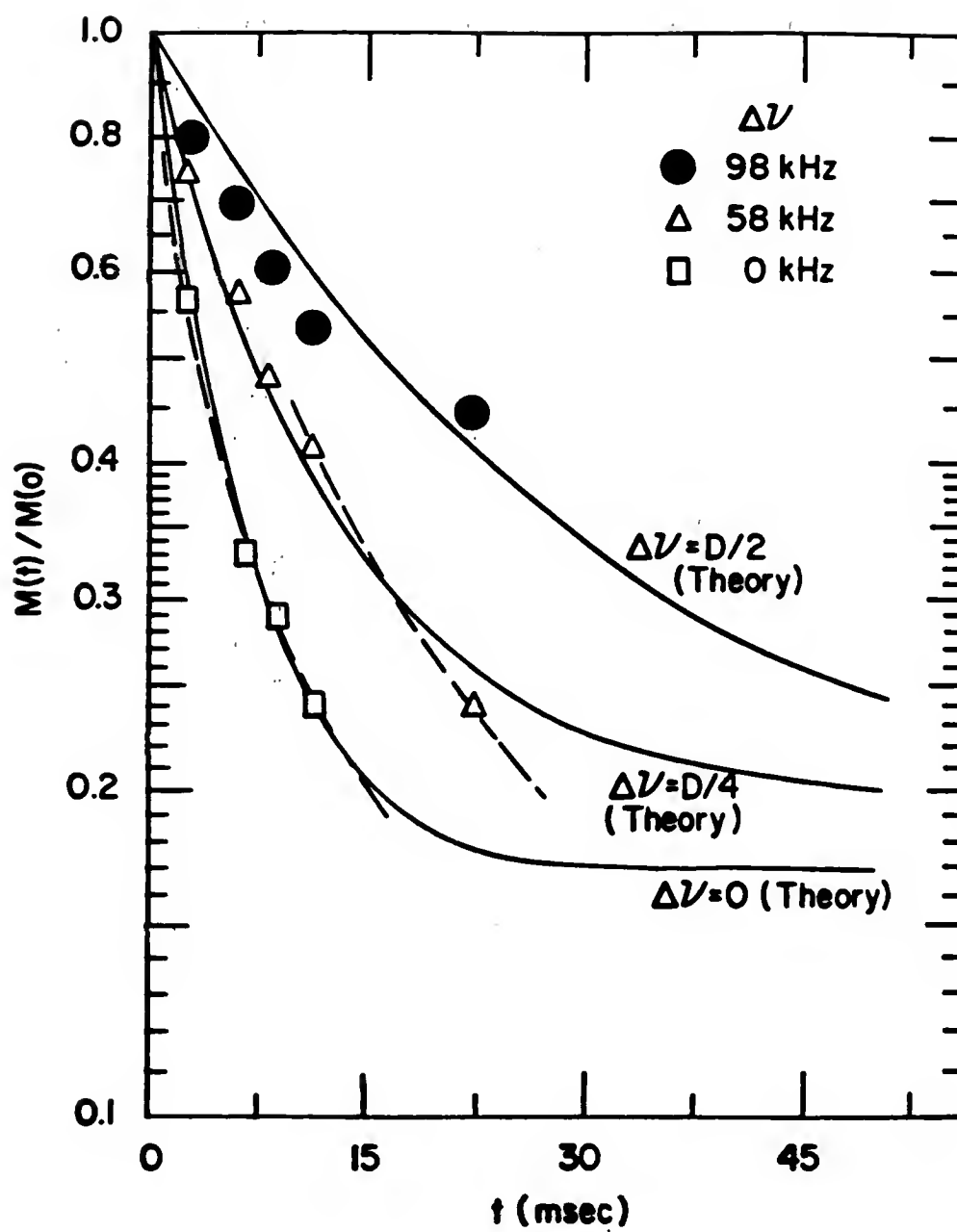
[a]Rates given in units of $\frac{D^2}{24\omega_0^2\tau}$

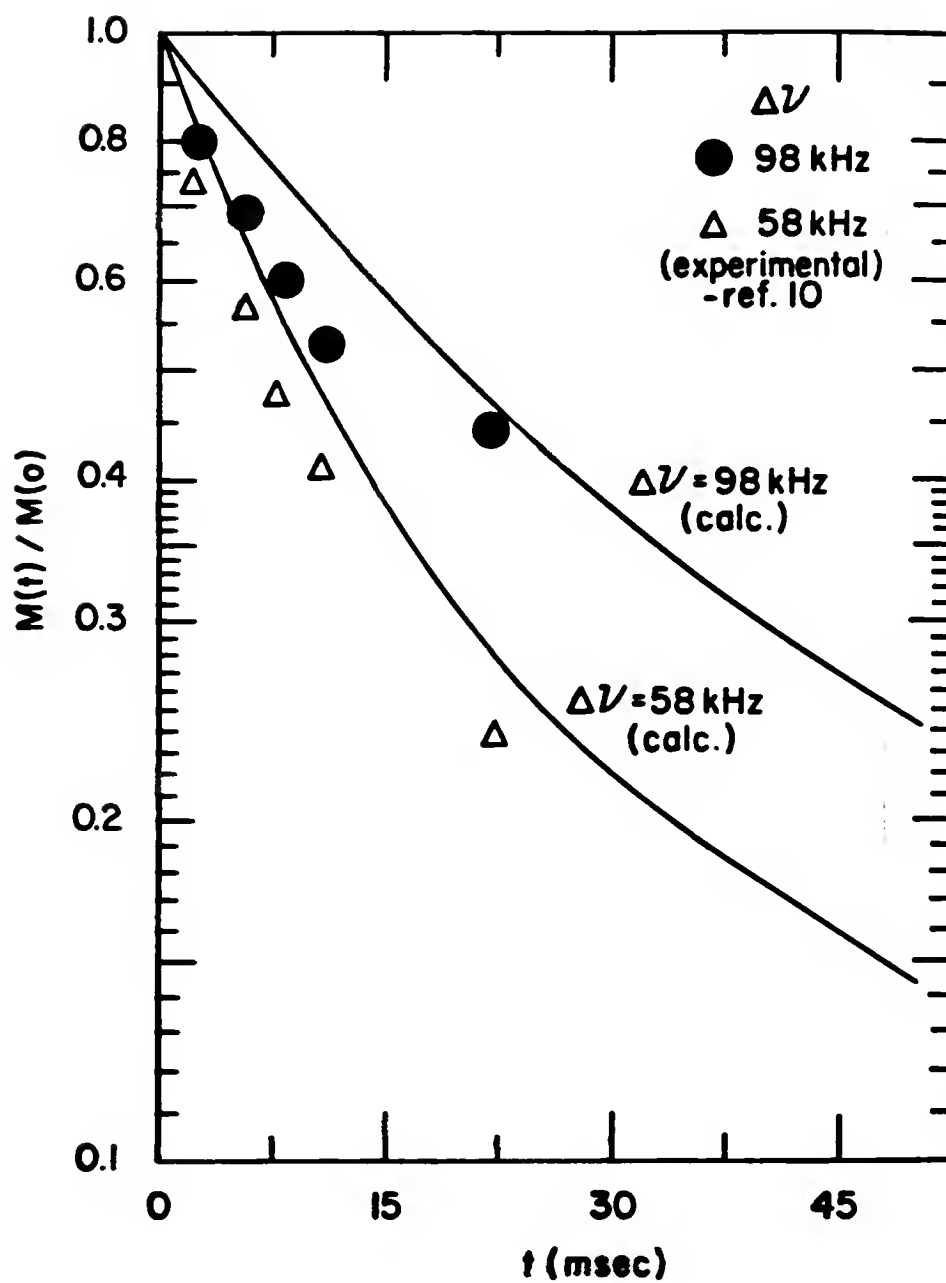Figure 9. Time Dependence of M(t) for Different $\Delta\nu$

Figure 10. Time Dependence of M(t) for
$\Delta \nu = 98$ and $\Delta \nu = 58$ khz

CHAPTER 4

ORIENTATIONAL ORDER PARAMETERS

Density Matrix Formalism

A particle (e.g., an atom, molecule or nucleus) isolated in space and with nonzero angular momentum in its rest frame has a manifold of states with equal energy. The problem is how to specify the orientational degrees of freedom of an individual molecule. We describe the degrees of freedom of the quantum rotors with angular momentum $J = 1$ in terms of single particle 3×3 density matrices ρ_i (for each site i). The ρ_i are completely described by

(1) the molecular dipole mements $\langle J_x \rangle_i$, $\langle J_y \rangle_i$, $\langle J_z \rangle_i$ and

(2) the quadrupole moments $\langle J_z^2 \rangle_i$, $\langle J_x J_y \rangle_i$, $\langle J_y J_z \rangle_i$.... In the absence of interactions which break time reversal symmetry, the dipole moments $\langle J_x \rangle$, $\langle J_y \rangle$, and $\langle J_z \rangle$ vanish and we need only consider 5 independent variables.

Instead of Cartesian components, it is more convenient to use a set of irreducible tensorial operatiors Π_{LM} with $0 \leq L \leq 2J$ for general J and the associated multipole moments

$$t_{lm} = Tr(\rho \Pi_{lm}) \tag{4.1}$$

For simplicity the site index has been dropped. The expansion of the single particle density operator in terms of the multipole moments is given by

$$\rho = \frac{1}{(2J+1)} \sum_{L=0}^{2J} \sum_{M=-L}^{L} (2L+1) t_{LM}^* \Pi_{LM} \tag{4.2}$$

There are three conditions imposed on ρ: Hermiticity and both weak and strong positivity conditions(34).

ρ is a Hermitian operator and

$$t_{LM} = (-1)^M t^*_{L-M} \tag{4.3}$$

Π_{oo} is a unit matrix operator and $t_{oo} = 1 = Tr\rho$

The weak positivity conditions are given by

$$\frac{1}{2J+1} \le Tr(\rho^2) \le 1 \tag{4.4}$$

When one eigenvalue is equal to 1, the others being null; then the matrix ρ describes a pure state and $Tr(\rho^2) = 1$. The minimum of $Tr(\rho^2)$ is reached when all the eigenvalues are equal to $(2J+1)^{-1}$; then the matrix describes a completely unpolarized state and $Tr(\rho^2) = (2J+1)^{-1}$.

For density matrices of spin$-\frac{1}{2}$ particles, condition (4.4) is the only condition imposed by the positivity condition. But for $J > \frac{1}{2}$, further conditions are imposed on the density matrix and on the multipole parameters by the positivity property.

The eigenvalues of ρ must be positive definite because they represent the probabilities of realizing some given state and this leads to the strong positivity conditions

$$0 \le \lambda_n \le 1 \tag{4.5}$$

where λ_n is the nth eigenvalue. These conditions place the strongest limitations on the allowed values for the multipole moments and thus on the allowed values of the local order parameters for ortho-H_2 molecules in the solid mixtures.

It is useful to construct orthonormal matrix representations of the irreducible operators Π_{LM} in the representation (J^2, J_z). For J=1 these are given

by the following 3×3 matrix operators with rows (and columns) labelled by the eigenvalues $1, 0, -1$ of J_z.

$$\Pi_{10} = \frac{1}{\sqrt{2}} J_Z = \frac{1}{\sqrt{2}} \begin{pmatrix} 1 & 0 & 0 \\ 0 & 0 & 0 \\ 0 & 0 & -1 \end{pmatrix}$$

$$\Pi_{11} = -\frac{1}{\sqrt{2}} J_+ = -\frac{1}{\sqrt{2}} \begin{pmatrix} 0 & 1 & 0 \\ 0 & 0 & 1 \\ 0 & 0 & 0 \end{pmatrix}$$

$$\Pi_{20} = \frac{1}{\sqrt{6}} (3J_z^2 - J^2) = \frac{1}{\sqrt{6}} \begin{pmatrix} 1 & 0 & 0 \\ 0 & -2 & 0 \\ 0 & 0 & 1 \end{pmatrix} \tag{4.6}$$

$$\Pi_{21} = -\frac{1}{2} (J_z J_+ + J_+ J_z) = -\frac{1}{\sqrt{2}} \begin{pmatrix} 0 & 1 & 0 \\ 0 & 0 & -1 \\ 0 & 0 & 0 \end{pmatrix}$$

$$\Pi_{22} = \frac{1}{2} J_+^2 = \begin{pmatrix} 0 & 0 & 1 \\ 0 & 0 & 0 \\ 0 & 0 & 0 \end{pmatrix} \tag{4.7}$$

$$\Pi_{L,M} = (-1)^M \Pi_{L,-M}^{\dagger} \tag{4.8}$$

and

$$Tr(\Pi_{LM} \Pi_{L'M'}^{\dagger}) = \delta_{LL'} \delta_{MM'} \tag{4.9}$$

The quadrupole operators Π_{2M} transform analogously to the spherical harmonics $Y_{2m}(\alpha, \beta)$ with respect to rotations of the coordinate axes.

The reference axes have remained arbitrary in the discussion and we are therefore free to choose local references axes that correspond to the local symmetry for each molecule. The natural choice for the z-axis is along the net component of the angular momentum at a given site, i.e. such that $\langle J_x \rangle = \langle J_x \rangle = 0$.

The general form for $\rho_{J=1}$ can be identified by the mean values of its magnetic dipole and electric quadrupole mements in the above notation:

$$\rho = \frac{1}{3} \Pi_3 + \sum_n \mu_n \Pi_n + \sum_m Q_m \Pi_{2m} \tag{4.10}$$

where $\mu_n = \langle \Pi_{1n}^{\dagger} \rangle$ and $Q_m = \langle \Pi_{2m}^{\dagger} \rangle$

The expression (4.10) is identical with that was derived by ref.35 and ref.73.

We still can choose x and y axes such that Q_2 is real. i.e.

$$Q_2 = \frac{1}{2}\langle J_x^2 - J_y^2 \rangle \tag{4.11}$$

and

$$\langle J_x J_y + J_y J_x \rangle = 0 \tag{4.12}$$

Q_2 measures the departure from axial symmetry about the z axis and is sometimes called the eccentricity (29, 30). It can be shown that with this choice of local reference frame Q_1 and Q_{-1} also vanish and the density matrix may be written as

$$\rho = \frac{1}{3}\Pi_3 + \frac{1}{\sqrt{2}}\mu_0 \begin{pmatrix} 1 & 0 & 0 \\ 0 & 0 & 0 \\ 0 & 0 & -1 \end{pmatrix} + \begin{pmatrix} \frac{1}{\sqrt{6}}Q_0 & 0 & Q_2 \\ 0 & \frac{-2}{\sqrt{6}}Q_0 & 0 \\ Q_2 & 0 & \frac{1}{\sqrt{6}}Q_0 \end{pmatrix} \tag{4.13}$$

where

$$\mu_0 = \frac{1}{\sqrt{2}}\langle J_z \rangle$$

$$Q_0 = \frac{1}{\sqrt{6}}\langle (3J_z^2 - 2) \rangle \tag{4.14}$$

Q_0 is the alignment (29, 30) along the z-axis. Sometimes it is convenient to define the alignment and the eccentricity as

$$\sigma' = \langle 1 - \frac{3}{2}J_z^2 \rangle = -\sqrt{\frac{3}{2}}Q_0 \tag{4.15}$$

$$\eta = \langle J_x^2 - J_y^2 \rangle = 2Q_2 \tag{4.16}$$

Both σ' and η have maximum amplitude of unity. In terms of these parameters ρ becomes

$$\rho = \frac{1}{3}\Pi_3 + \frac{1}{2}\mu \begin{pmatrix} 1 & 0 & 0 \\ 0 & 0 & 1 \\ 0 & 0 & -1 \end{pmatrix} + \begin{pmatrix} -\frac{1}{3}\sigma' & 0 & \frac{1}{2}\eta \\ 0 & \frac{2}{3}\sigma' & 0 \\ \frac{1}{2}\eta & 0 & -\frac{1}{3}\sigma' \end{pmatrix} \tag{4.17}$$
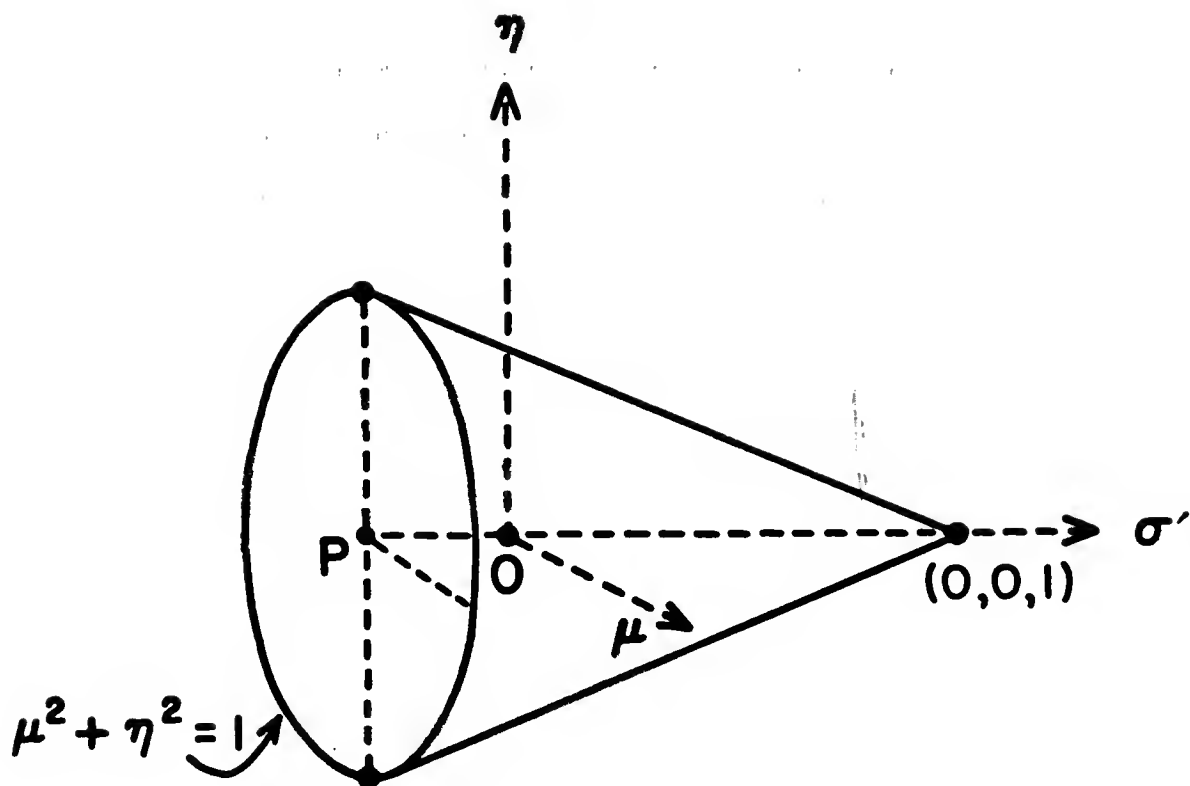
Figure 11. The Allowed Values of $\mu = \langle J_z \rangle$,
σ And η for Spin-1 Particle

where $\mu = \langle J_z \rangle$.

The three eigenvalues of ρ are

$$\lambda_1 = \frac{1}{3} + \frac{2}{3}\sigma'$$

$$\lambda_{2,(3)} = \frac{1}{3} - \frac{1}{3}\sigma' \pm \frac{1}{2}\sqrt{\mu^2 + \eta^2} \tag{4.18}$$

The strong positivity conditions, $\lambda_n \geq 0$, are therefore seen to restrict the allowed values of the local order parameters σ', η and μ to the interior of a cone (Fig.11) in the 3D parameter space. The vertex of the cone is located at $\sigma' = 1$, $\mu = \eta = 0$, corresponding to the pure state $\mid \psi \rangle = \mid J_z = 0 \rangle$, and the base of the cone is defined by $\sigma' = -\frac{1}{2}$ and $\mu^2 + \eta^2 = 1$ which corresponds to the pure state $\mid \psi \rangle = cos\gamma \mid J_z = 1 \rangle + sin\gamma \mid J_z = -1 \rangle$ with $\langle J_z \rangle = cos2\gamma$ and $\langle J_+^2 \rangle = sin2\gamma$ (The polar angle γ generates the points on the circle of the cone's baseplate).

The positivity domain shown in Fig.11 is the same as those obtained by Minnaert (34) using the Ebhard-Good theorem and similar to those given by W.Lakin (32) in his analysis of the states of polarization of the deuteron. Having established the physical considerations which determine the limited range of allowed values for the order parameters, we now turn to the special case of solid hydrogen.

Applications to Solid Hydrogen

In the absence of interactions which break time reversal symmetry, the expectation value $\langle J_\alpha \rangle$ must vanish for all α in solid hydrogen. This is the so-called "quenching" of the orbital angular momentum (74). The reason for this is that in the solid the electronic distribution of a given molecule may (to a first approximation) be regarded as being in an inhomogeneous electric

field which represents the effect of the other molecules. This inhomogeneity removes the spatial degeneracy of the molecular wave function which must be real and the expectation value of the orbital angular momentum $\langle i\hbar\frac{\partial}{\partial\phi}\rangle$ must accordingly vanish. The separation of the rotational energy levels is given by $E_J = BJ(J+1)$ with B=85.37K, and in the solid at low temperatures only the lowest J values, $J = 0$ for para-H_2 and $J = 1$ for ortho-H_2, need be considered.

At low temperatures the anisotropic forces between the ortho molecules lift the rotational degeneracy and the molecules align themselves with respect to one another to minimize their interaction energy. For high ortho concentrations one observes a periodic alignment in a Pa_3 configuration with four interpenetrating simple cubic sub-lattices, the molecules being aligned parallel to a given body diagonal in each sub-lattice and the order parameters, $\sigma'_\alpha = \langle 1 - \frac{3}{2}J_{z\alpha}^2 \rangle$, are the same at each site $\sigma'_\alpha = 1$.

The long range periodic order for the molecular alignments is lost below a critical concentration of approximately 55% and the NMR studies indicate that there is only short range orientational ordering with a broad distribution of local symmetry axes and local order parameters throughout the sample. This purely local ordering has been referred to as a quadrupolar glass in analogy with the spin glasses, but unlike the dipolar spin glasses, there is no well-defined transition from the disordered state to the glass regime. In order to describe the ortho molecules in the glass regime, where there is a large number of sites with various values of σ', a density matrix formalism must be used.

The quenching of the angular momentum in solid H_2 has two consequences for the limits on the allowed values for the order paramters:

(1) From the previous discussion, the allowed values of σ' and η lie within a triangle bounded by the three lines (Fig.12 $\triangle ABC$).

$$\frac{1}{3} + \frac{2}{3}\sigma' \geq 0$$

$$\frac{1}{3} - \frac{1}{3}\sigma' \pm \frac{1}{2}\eta \geq 0 \qquad (4.19)$$

which represent the strong positivity conditions for the eigenvalues of ρ when the angular momentum is quenched.

(2) Since $\langle J_\alpha \rangle = 0$ for all α, we are free to choose the z-axis which was previously fixed by the net component of the angular momentum. The natural choice for the local reference axes is now the set of principal axes for the quadrupolar tensor

$$Q_{\alpha\beta} = \langle \frac{1}{2}(J_\alpha J_\beta + J_\beta J_\alpha) - \frac{1}{3}J^2 \delta_{\alpha\beta} \rangle \qquad (4.20)$$

The choice of principal axes is not unique, however, because after finding one set we can always find another five by relabeling axes. We can prove that not all of the points in the "allowed" portion of the (σ', η) plane are inequivalent (every point represents one state), and we only need to consider the hatched region (triangle CFE) in Fig.12. The states of all other areas of the triangle of allowed values can be obtained from the $\triangle CFE$ by suitable rotations (i.e. relabel the axes).

The important point is that the pure states

$$\psi_C = | J_z = 0 \rangle \qquad (4.21)$$

and

$$\psi_A = \frac{1}{\sqrt{2}}(| J_z = 1 \rangle + | J_z = -1 \rangle) \qquad (4.22)$$

are not inequivalent (The labels A through F refer to the special points on the triangle of allowed values shown in Fig.12), and the corresponding wave functions are listed in Table VI. The state ψ_A can be obtained from ψ_C by a rotation of the axes by $\frac{3\pi}{2}$ about x axis.

The rotation operator

$$R_x(\frac{3\pi}{2}) = exp(-\frac{i}{\hbar}\frac{3\pi}{2}J_x) = -(\frac{J_x}{\hbar})^2 + i(\frac{J_x}{\hbar}) + I \qquad (4.23)$$

and

$$R_x(\frac{3\pi}{2})\psi_C = e^{i\frac{\pi}{2}}\psi_A \qquad (4.24)$$

The rotation $R_x(\frac{3\pi}{2})$ leaves the state F invariant and maps D onto the point G in parameter space.

We can furthermore show that the rotation $R_x(\frac{3\pi}{2})$ maps the following triangular regions of parameter space onto one another

$$\triangle CDF \rightarrow \triangle AGF$$

$$\triangle CEF \rightarrow \triangle AEF$$

and

$$\triangle BDF \rightarrow \triangle BGF \qquad (4.25)$$

It is also seen by considering the transformation

$$\rho'(\sigma'',\eta') = R_x^{\dagger}(\frac{3\pi}{2})\rho(\sigma',\eta)R_x(\frac{3\pi}{2}) \qquad (4.26)$$

using the matrix representation

$$R_x(\frac{3\pi}{2}) = \begin{pmatrix} \frac{1}{2} & \frac{i}{\sqrt{2}} & -\frac{1}{2} \\ \frac{i}{\sqrt{2}} & 0 & \frac{i}{\sqrt{2}} \\ -\frac{1}{2} & \frac{i}{\sqrt{2}} & \frac{1}{2} \end{pmatrix} \qquad (4.27)$$

Table VI Special Points in Orientational Order Parameter Space. (see Fig.12)

Label	parame.	Wave Function	
A	$(-\frac{1}{2},1)$	$[\mid 1\rangle + \mid -1\rangle]/\sqrt{2}$	
B	$(-\frac{1}{2},-1)$	$[\mid 1\rangle - \mid -1\rangle/\sqrt{2}$	
C	$(1,0)$	$\mid 0\rangle$	
D	$(\frac{1}{4},-\frac{1}{2})$	$[\mid 1\rangle - \mid -1\rangle - \sqrt{2}\mid 0\rangle]/2$	
E	$(\frac{1}{4},\frac{1}{2})$	$[i(\mid 1\rangle + \mid -1\rangle) - \sqrt{2}\mid 0\rangle]/2$	
F	$(0,0)$	$[(-1+i)\mid 1\rangle + (1+i)\mid -1\rangle - \sqrt{2}\mid 0\rangle]/\sqrt{6}$	
G	$(-\frac{1}{2},0)$	$[(-1+i)\mid 1\rangle + (1+i)\mid -1\rangle]/2$	

$R_x(\frac{3\pi}{2}) : \psi_C \to \psi_A, \psi_D \to \psi_G; \psi_B, \psi_F, \psi_E$ fixed.

$R_z(\frac{\pi}{2}) : \psi_A \to \psi_B, \Psi_E \to \psi_D; \psi_C, \psi_F, \psi_G$ fixed.

The $R_x(\frac{3\pi}{2})$ transforms the points (σ', η) into new points (σ'', η') given by

$$\begin{pmatrix} \sigma'' \\ \eta' \end{pmatrix} = \begin{pmatrix} -\frac{1}{2} & \frac{3}{4} \\ 1 & \frac{1}{2} \end{pmatrix} \begin{pmatrix} \sigma' \\ \eta \end{pmatrix} \tag{4.28}$$

which corresponds to the mapping given by eqs.(4.25).

There is some confusion in the literature concerning the values of σ'. In Van Kranendonk's(75) book the negative value of σ' had been ruled out as it was unphysical. But this is not strictly correct. Van Kranendonk's remarks refer to considerations of the pure states $\mid J_z = 0\rangle$ and $\mid J_z = \pm 1\rangle$ only. He does not discuss either the density matrix approach or the formulation of the intrinsic quadrupolar order parameters σ' and η needed to describe the orientational degrees of freedom of the ortho-H_2 molecules.

The results of the relabeling transformation are particularly easy to understand if we consider the pair $(S = \sigma', N = \frac{\sqrt{3}}{2}\eta)$ which transform orthonormally when the axes are rotated. The parameter space (S, N) is shown in

Fig.13. The rotation $R_x(\frac{3\pi}{2})$ in (S, N) parameter space through the line BZ with the transformed points given by

$$\begin{pmatrix} S' \\ N' \end{pmatrix} = \begin{pmatrix} -\frac{1}{2} & \frac{\sqrt{3}}{2} \\ \frac{\sqrt{3}}{2} & \frac{1}{2} \end{pmatrix} \begin{pmatrix} S \\ N \end{pmatrix} \tag{4.29}$$

Similarly, the relabeling $(x, y, z) \to (y, x, z)$ corresponds to a reflection through the line CG. The entire area of allowed values in parameter space can therefore be mapped out starting only with the triangle $\triangle CFE$ by simply relabelling the principal axes. We only need to consider the hatched region of parameter space shown in Fig.12 in order to describe all physically distinguishable orientational states for ortho-H_2 molecules in the solid state. This is not the only choice that can be made for a "primitive" area of inequivalent values of (σ', η). We may also choose the sum of $\triangle CFK$ and $\triangle GFJ$ in Fig.13. In that region the states have the minimum values of the eccentricity N. Both choices are equivalent.

A Proposition for A Zero Field Experiment

An equivalent expression for the spectrum for each molecule is

$$\triangle\nu_i = \pm\sqrt{\frac{3}{2}}D\langle\pi_{20(i)}\rangle_{OZ} \tag{4.30}$$

As previously discussed, considering the transformation to the local frame we obtained

$$\triangle\nu_i = \pm D[-\sigma'_i p_2(cos\theta_i) + \frac{3}{4}\eta_i sin^2\theta_i cos2\phi_i] \tag{4.31}$$

where (θ_i, ϕ_i) are the polar angles defining the orientation of the applied magnetic field with respect to the local molecular symmetry axes.
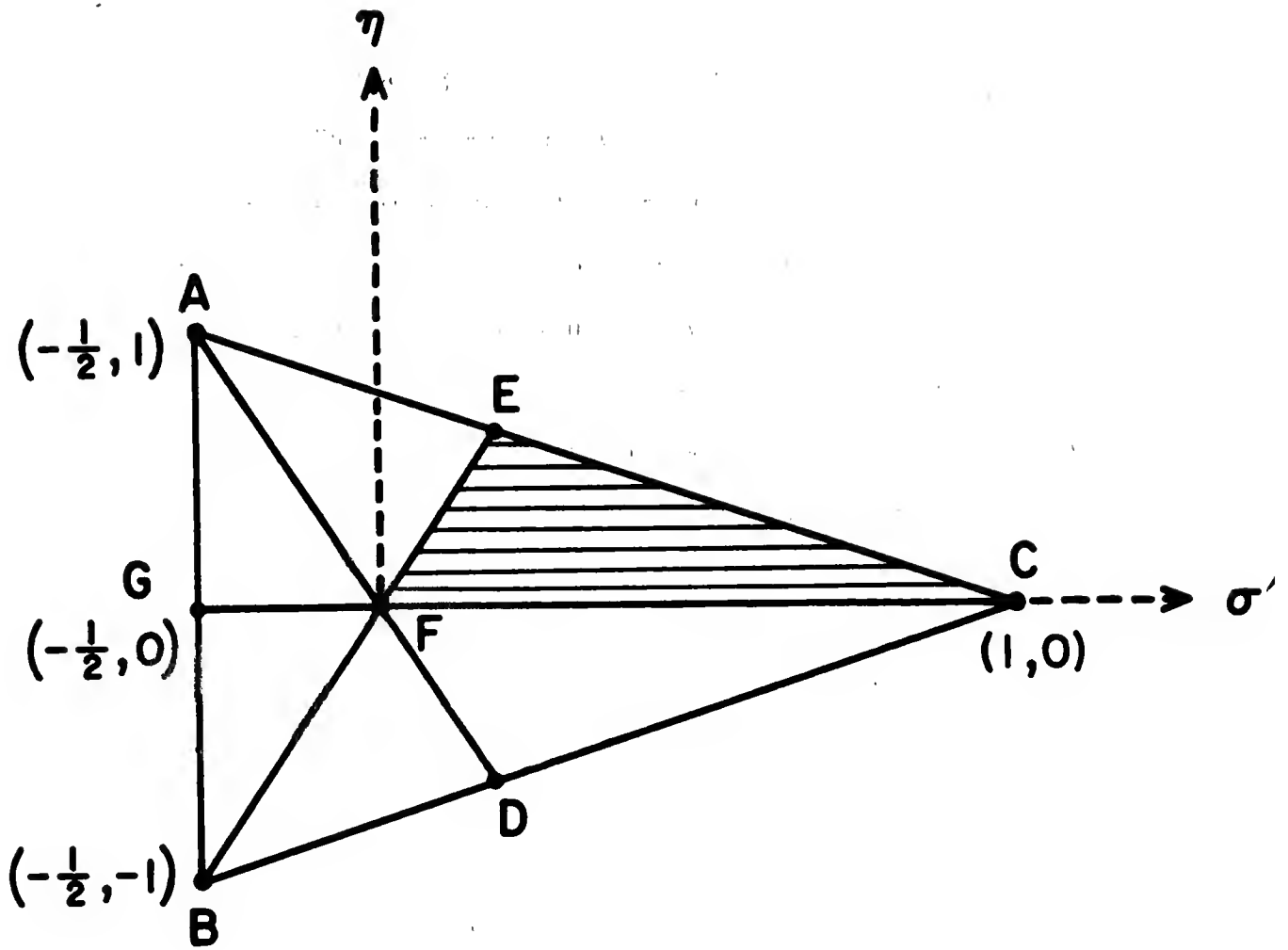
Figure 12. The Allowed Values of σ And η
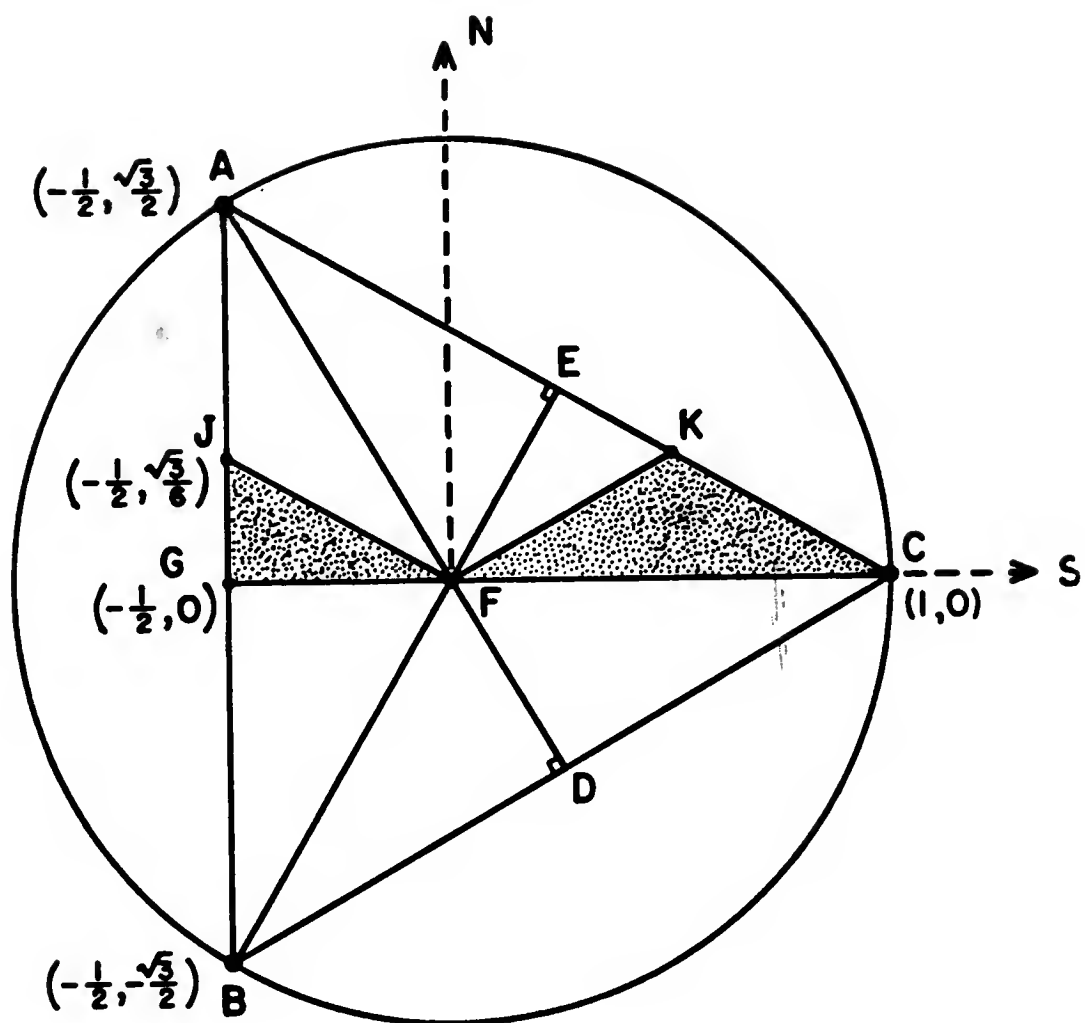for Spin-1 Particle

Figure 13. Diagram of Allowed S And N

We propose that the assumption of axial symmetry can be tested experimentally by examining the zero field NMR absorption spectrum. Reif and Purcell (76) have carried out zero field studies for the long range ordered phase where it is known that σ' is constant and $\eta = 0$, but it has not previously been considered for the glass phase.

In zero applied magnetic field the degeneracy of the nuclear spin levels is lifted only by the intramolecular spin-spin interactions.

$$H_{DD}(i) = hD[-\frac{1}{3}\sigma_i'(3I_{zi}^2 - I_i^2) + \frac{1}{4}\eta_i(I_{+i}^2 + I_{-i}^2)] \qquad (4.32)$$

The tensorial operators for the rotational degrees of freedom have been replaced by the expectation values σ' and η. An applied radio-frequency field can induce magnetic dipole transitions between the nuclear spin levels in analogy with the so-called pure quadrupole resonance absorption(51 Chapter VIII). The eigenstates of H_{DD} are $| I_Z = 0\rangle$ and $| \pm\rangle = \frac{1}{\sqrt{2}}(| I_z = 1\rangle \pm | I_z = -1\rangle$. For each molecule i, three resonance lines can be expected corresponding to the transitions $| +\rangle \rightarrow | 0\rangle, | -\rangle \rightarrow | 0\rangle$ and $| +\rangle \rightarrow | -\rangle$ with frequencies $\nu_i^1 = D(-\sigma_i' + \frac{1}{2}\eta_i)$, $\nu_i^2 = D(-\sigma_i' - \frac{1}{2}\eta_i)$ and $\nu_i^3 = D\eta_i$, respectively. If axial symmetry is a good approximation, there is only one line at $\nu_i = -D\sigma_i'$ and the detailed shape of the NMR absorption spectrum in zero field will be identical with that observed at high fields. Otherwise the high and zero field spectra will not be identical.

A Model for The Distribution Function of σ

X. Li, H. Meyer and A. J. Berlinsky (23) have proposed a model for the distribution function of σ'. They assume that for a single crystal the orientation

of the principal axes are uniformly distributed. They considered a Cartesian basis for the description of the single particle density matrices

$$\rho_i^x = \frac{1}{2}\langle - J_{x_i}^2 + J_{y_i}^2 + J_{z_i}^2 \rangle$$

$$\rho_i^y = \frac{1}{2}\langle J_{x_i}^2 - J_{y_i}^2 + J_{z_i}^2 \rangle$$

$$\rho_i^z = \langle 1 - J_{z_i}^2 \rangle = \frac{1}{2}\langle J_{x_i}^2 + J_{y_i}^2 - J_{z_i}^2 \rangle$$

The pure states $\rho_i^{(\alpha)} = 1$ correspond to ψ_α-wave functions for $\alpha = x, y, \text{or } z$. This leads to a natural parameterization of the $\rho_i^{(\alpha)}$ given by

$$\rho_i^{(\alpha)} = \frac{e^{-\beta E_{\alpha_i}}}{\sum_\alpha e^{-\beta E_{\alpha_i}}}$$

where the "energies" E_{α_i} are in general temperature dependent. Li et al (23) then made the further assumption that the effective site energies are normally distributed about zero with a width $\Delta(T)$ subject to the constraint $\sum_\alpha E_{\alpha_i} = 0$. i.e.

$$P(E_x, E_y, E_z) = -\frac{\sqrt{3}}{2\pi\Delta^2} e^{-\frac{1}{2}(E_x^2 + E_y^2 + E_z^2)/\Delta^2} \delta(E_x + E_y + E_z)$$

These assumptions lead to definite predictions concerning the variation of the NMR line shape parameters M_2 and M_4, and in particular of the variation of $\frac{M_4}{M_2^2}$ as a function of the degree of local orientational order parameter measured by $(\sigma_{eff})_{rms}$.

Instead of Cartesian symmetry for the effective site energies, we explored the same trends for a cylindrical symmetry for the effective site energies because of the axial symmetry of the quadrupolar interactions. This also leads to a natural description of the energy states in terms of local "two level system," corresponding to $J_{z_i} = \pm 1$ and $J_{z_i} = 0$ separeted by an energy gap Δ_i.

The probability distribution of Δ is Gaussian as following

$$P(\Delta) = \sqrt{\frac{2}{\pi D^2}} e^{-\frac{\Delta^2}{2D^2}} \tag{4.33}$$

The order parameter $\sigma = \langle 3J_z^2 - 2 \rangle$ will be

$$\langle \sigma(\Delta) \rangle = \frac{2e^{-\frac{\Delta}{KT}} - 2}{2e^{-\frac{\Delta}{KT}} + 1} \tag{4.34}$$

We can prove that

$$\frac{M_4}{M_2^2} = \frac{15}{7} \frac{\langle \sigma^4 \rangle}{(\langle \sigma^2 \rangle)^2} \tag{4.35}$$

where

$$\langle \sigma^2 \rangle = \int_0^\infty \frac{(2e^{-\frac{\Delta}{KT}} - 2)^2}{(2e^{-\frac{\Delta}{KT}} + 1)^2} \sqrt{\frac{2}{\pi D^2}} e^{-\Delta^2} \, d\Delta \tag{4.36}$$

let $\frac{\Delta}{D} = X$

$$\langle \sigma^2 \rangle = \int_0^\infty \frac{(2e^{-\frac{D}{KT}X} - 2)^2}{(2e^{-\frac{D}{KT}X} + 1)^2} \sqrt{\frac{2}{\pi}} e^{\frac{-X^2}{2}} \, dX \tag{4.37}$$

$$\langle \sigma^4 \rangle = \int_0^\infty \frac{(2e^{-\frac{D}{KT}X} - 2)^4}{(2e^{-\frac{D}{KT}X} + 1)^4} \sqrt{\frac{2}{\pi}} e^{\frac{-X^2}{2}} \, dX \tag{4.38}$$

By using numerical integral method the curve in Fig.14 shows the ratio $\frac{\langle \sigma^4 \rangle}{\langle \sigma^2 \rangle^2}$ versus $\sqrt{\langle \sigma^2 \rangle}$(order).

Considering the intermolecular and the intramolecular dipolar broadening, the fourth moment M_4 and the second mement M_2 should be (51)

$$M_2 = -\frac{Tr\{[\mathcal{H}_1', I_x]^2\}}{Tr\{I_x^2\}} \tag{4.39}$$

$$M_4 = \frac{Tr\{[\mathcal{H}_1', [\mathcal{H}_1', I_x]]^2\}}{Tr\{I_x^2\}} \tag{4.40}$$

where

$$\mathcal{H}_1' = \mathcal{H}_1^{intra} + \mathcal{H}_1^{inter}$$

$$\mathcal{H}_1^{intra} = \frac{1}{4}\gamma_I^2 \hbar \sum_{k,l} \frac{1 - 3\cos^2\theta_{kl}}{r_{kl}^3}(3I_z^k I_z^l - \vec{I}^k \cdot \vec{I}^l)$$

$$\mathcal{H}_1^{inter} = \gamma_i \gamma_s \hbar \sum_{i,j} \frac{(1 - 3cos^2\theta_{ij})}{r_{ij}^3} I_z^i S_z^j$$

Following a quite complicated but straightforward calculation we can prove that

$$M_2 = M_2^{intra} + M_2^{inter} \tag{4.41}$$

$$M_4 = M_4^{intra} + M_4^{inter} + 4M_2^{intra}M_2^{inter} \tag{4.42}$$

For a Gaussian shape one has $M_4^{inter} = 3(M_2^{inter})^2$ and

$$M_4 = M_4^{intra} + 3(M_2^{inter})^2 + 4M_2^{intra}M_2^{inter} \tag{4.43}$$

Taking the same value of $M_2^{inter} = 20(khz)^2$ as in ref.23 we obtain the curve in Fig.15. The upper one is $\frac{M_4^{intra}}{(M_2^{intra})^2}$ versus $\sqrt{\langle\sigma^2\rangle}$ and the lower one is $\frac{M_4}{(M_2)^2}$ versus $\sqrt{\langle\sigma^2\rangle}$.

The experimental lineshapes (23,24,27) are below the calculated lineshape, but the shape and slope are almost the same. The value of maximum $\frac{M_4}{M_2^2}$ of experimental lineshape is 3.15 (18) and the value of maximum $\frac{M_4}{M_2^2}$ of calculated lineshape is 5.60.
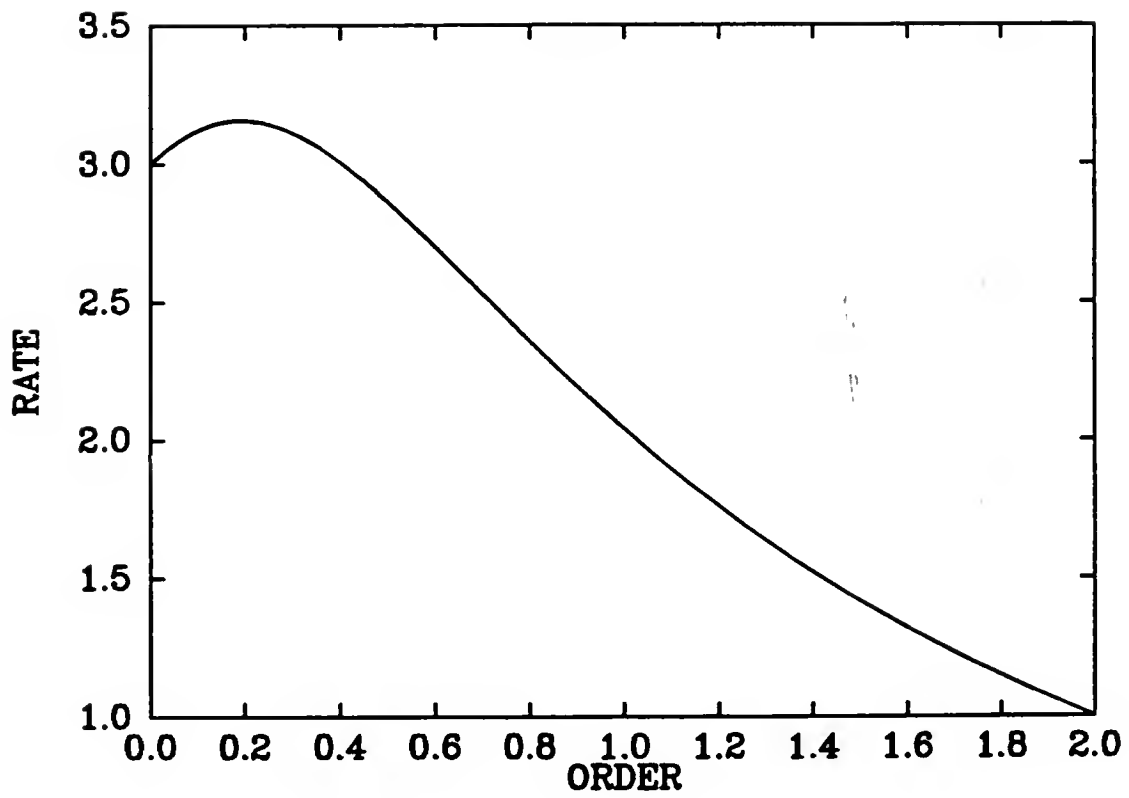
MODEL (INTRA)

Figure 14. Diagram of
$$\frac{\langle \sigma^4 \rangle}{\langle \sigma^2 \rangle^2}$$
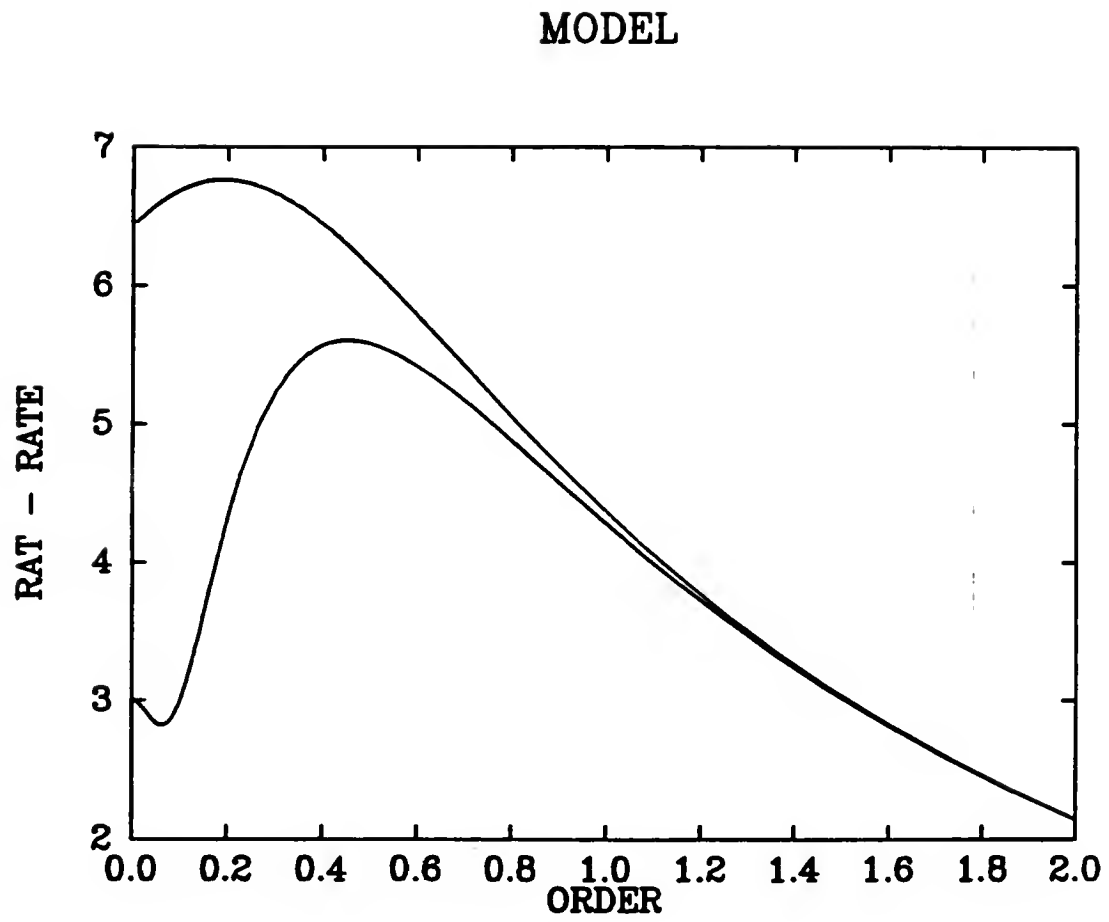versus $\sqrt{\langle \sigma^2 \rangle}$

MODEL

Figure 15. Diagram of $\frac{M_4}{(M_2)^2}$ versus order

CHAPTER 5

NMR PULSE STUDIES OF SOLID HYDROGEN

The experimental technique of nuclear magnetic resonance with spin echoes has been used widely in recent years as a tool to investigate the dynamical properties of crystals. In particular, much attention has been paid to the study of relaxation rates of dynamical processes in molecular solids by means of the spin echoes occuring after application of resonant rf $90° - \tau - \psi_{(\phi)}$ pulse sequences and rf $90° - \tau - \psi_{(\phi)} - t_w - \psi'_{(\phi')}$ pulse sequences.

The purpose of this chapter is to develop the theory of spin echoes of solid H_2 in orientationally ordered phase and discuss the low-frequency dynamics of orientational glasses.

Solid Echoes

There are several publications which have presented calculations for the amplitude of solid echo responses to $90° - \tau - \psi_\phi$ pulse sequences (39, 78, 79).

We would like to examine the time dependence of the nuclear operators and the conditions for the focussing of solid echoes.

The Time Dependence of The Nuclear Operators

A general two-pulse sequence denoted by $\left(\frac{\pi}{2} - \tau - \psi_\phi\right)$ is sketched in Fig.16.

In NMR experiments one observes only the ortho-molecules $(I = 1)$. In a first approximation we will treat the system as a set of independent molecules. The signal we measured is proportional to $Tr[\rho(t)I_+] = Tr[\rho(t)(I_x + iI_y)]$, where ρ is the density operator at time t and $\vec{I}$ the nuclear spin operator.
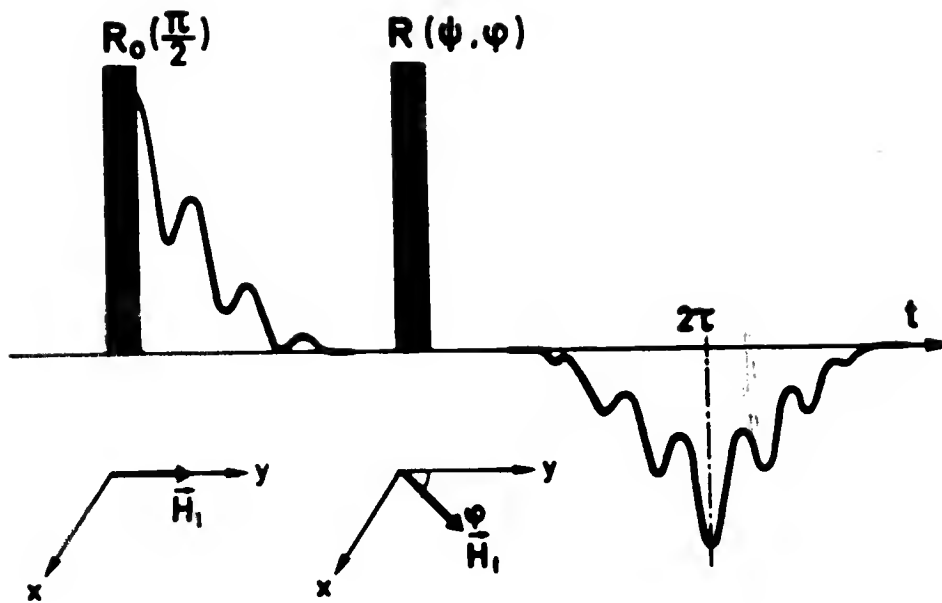
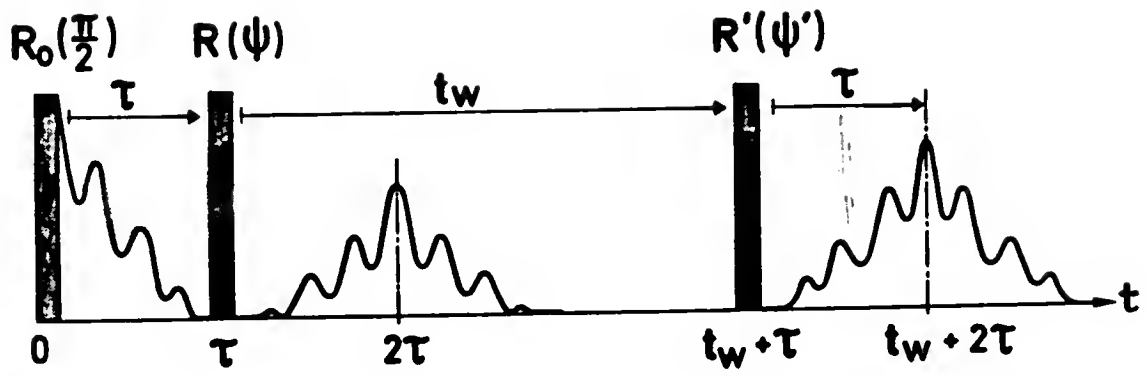Figure 16. Solid Echo (two-pulse sequence)

Figure 17. Stimulated Echo (three-pulse sequence)

In equilibrium the expression of density matrix is given by

$$\rho_{ieq} = \frac{e^{-\beta \mathcal{H}_0}}{Tr(e^{-\beta \mathcal{H}_0})} \tag{5.1}$$

Let Z be the direction of applied magnetic field.

$$\mathcal{H}_{0_i} = -\omega_0 \hbar I_{zi}$$

where ω_o is the Larmor frequency.

Since $\frac{\hbar \omega_0}{KT} \ll 1$, $e^{\frac{\hbar \omega_0}{KT} I_{zi}} \approx 1 + \frac{\hbar \omega_0}{KT} I_{zi}$

$$\rho_{ieq} \approx \frac{(1 + \frac{\hbar \omega_0}{KT} I_{zi})}{Tr(1 + \frac{\hbar \omega_0}{KT} I_{zi})} \approx \frac{1}{3}(1 + \frac{\hbar \omega_0}{KT} I_{zi}) \tag{5.2}$$

We know that the radio frequency field is responsible for nonequilibrium behavior of the system.

In the rotating frame after the first 90° pulse, the density matrix $\rho(0_+)$ would be

$$\rho(0_+) = e^{-\frac{i}{\hbar} \int H_1 dt} \rho_i(0_-) e^{\frac{i}{\hbar} \int H_1 dt} \tag{5.3}$$

If the radio frequency field is in the y direction of the rotation frame, we obtained

$$\rho(0_+) = e^{\frac{i}{\hbar} \frac{\pi}{2} I_y} [\frac{1}{3}(1 + \frac{\hbar \omega_0}{KT} I_z)] e^{-\frac{i}{\hbar} \frac{\pi}{2} I_y}$$

$$\rho(0_+) = \frac{1}{3}(1 + \frac{\hbar \omega_0}{KT} I_x) \tag{5.4}$$

This represents that the first pulse R_o puts the magnetization along the $\hat{x}$ axis (for simplicity we have dropped the site index i).

We shall consider the time evolution of the nuclear spin operators under the effect of the intramolecular Hamiltonian in the rotating frame.

$$H_{dd}^{sec} = \sum_i -\hbar \Delta \omega I_{zi} + \sum_i \frac{1}{2}\sqrt{\frac{2}{3}} D \hbar P_2(\theta_i) \sigma_i I_{i0}^2 \tag{5.5}$$

where

$$\sigma_i = \langle 3J_{zi}^2 - 2 \rangle$$

$$I_{i0}^2 = \frac{1}{\sqrt{6}}(3I_{zi}^2 - 2)$$

and

$$\rho(\tau_-) = e^{-\frac{i}{\hbar}\int_0^\tau H_{dd}^{sec}(t')dt'}\frac{1}{3}(1 + \frac{\hbar\omega_0}{KT}I_x)e^{\frac{i}{\hbar}\int_0^\tau H_{dd}^{sec}(t')dt'} \qquad (5.6)$$

It is assumed that the second pulse is a $\psi-$ pulse and the phase of that is ϕ (the angle between radio frequency field and $\hat{y}$ axis in rotating frame). After the second pulse the density matrix is given by

$$\rho(\tau_+) = e^{i\psi(I_x sin\phi + I_y cos\phi)}\rho(\tau_-)e^{-i\psi(I_x sin\phi + I_y cos\phi)} \qquad (5.7)$$

The nuclear spin density matrix at time t after second pulse is therefore

$$\rho(t + \tau) = u(t)R(\phi)u(\tau)\frac{1}{3}(1 + \frac{\hbar\omega_0}{KT}I_x)u^\dagger(\tau)R^\dagger(\phi)u^\dagger(t) \qquad (5.8)$$

where

$$u(t) = e^{[i\triangle\omega I_z - i\frac{1}{6}DP_2(\theta)\sigma(3I_z^2 - 2)]t} \qquad (5.9)$$

$$R(\phi) = e^{i\psi(I_x sin\phi + I_y cos\phi)} \qquad (5.10)$$

$$u(\tau) = e^{[i\triangle\omega I_z - i\frac{1}{6}DP_2(\theta)\sigma(3I_z^2 - 2)]\tau} \qquad (5.11)$$

and the signal

$$S(t + \tau) \propto Tr\{\rho(t + \tau)I_+\}$$

$$Tr\{\rho(t + \tau)I_+\}$$

$$= \frac{1}{3}\frac{\hbar\omega_0}{KT}Tr\{u(t)R(\phi)u(\tau)I_x u^\dagger(\tau)R^\dagger(\phi)u^\dagger(t)I_+\}$$

$$= \frac{1}{3}\frac{\hbar\omega_0}{KT}\sum_{m_1-m_8}\langle m_1 \mid u(t) \mid m_2\rangle\langle m_2 \mid R(\phi) \mid m_3\rangle\langle m_3 \mid u(\tau) \mid m_4\rangle$$

$$\langle m_4 \mid I_x \mid m_5\rangle\langle m_5 \mid u^\dagger(\tau) \mid m_6\rangle\langle m_6 \mid R^\dagger(\phi) \mid m_7\rangle$$

$$\langle m_7 \mid u^\dagger(t) \mid m_8 \rangle \langle m_8 \mid I_+ \mid m_1 \rangle \qquad (5.12)$$

Formation of Solid Echoes

After a lengthy calculation the results of eq.(5.12) are still quite complicated (for general ϕ and ψ). For some special values of ϕ and ψ the results are the same as that in ref.39. We would like to give the results in some special conditions.

(1)$\psi = 0$ (apply one pulse)

$$Tr\{\rho(t)I_+\} = \frac{2}{3}\frac{\hbar\omega_0}{KT}e^{-i\Delta\omega t}cos[\frac{1}{2}DP_2(\theta)\sigma t] \qquad (5.13)$$

This is called the Free Induction Decay.

(2) $\phi = 0, \psi = \frac{\pi}{2}$ This is a $90^\circ_y - \tau - 90^\circ_y$ pulse sequence

$$Tr\{\rho(t+\tau)I_+\}$$

$$= \frac{1}{3}\frac{\hbar\omega_0}{KT}e^{-i\Delta\omega t}cos[\frac{1}{2}DP_2(\theta)\sigma(t-\tau)](1 - e^{i\Delta\omega 2\tau}) \qquad (5.14)$$

Obviously, $Tr\{\rho(t+\tau)I_+\}$ has a maximum value at $t = \tau$. This is what is the meant by a solid echo. Another question is that according to eq.(5.14) the in-phase echo ($\triangle\omega = 0$) does not exist. This is in disagreement with the experimental results. The reason lies in neglecting intermolecular dipole-dipole interaction and the difficulty of getting exact $\triangle\omega = 0$ in experiments.

(3)$\phi = \frac{\pi}{2}$, $\psi = \frac{\pi}{2}$ This is a $90^\circ_y - \tau - 90^\circ_x$ pulse sequence

$$Tr\{\rho(t+\tau)I_+\}$$

$$= \frac{1}{3}\frac{\hbar\omega_0}{KT}e^{-i\Delta\omega t}cos[\frac{1}{2}DP_2(\theta)\sigma(t-\tau)](1 + e^{i\Delta\omega 2\tau}) \qquad (5.15)$$

From eq.(5.15), same as the second case, $Tr\{\rho(t+\tau)I_+\}$ obtaines maximum value at $t = \tau$, forming the solid echo.

Stimulated Echoes

It is already shown that in certain cases a sequence of three 90° pulses may be advantageous (80,81).

We first describe the formation of nuclear spin stimulated echoes. The stimulated echoes can be used to compare a "fingerprint" of the local molecular orientations at a given time with those at some later time (less than T_1) and thereby used to detect ultra-slow molecular re-orientations.

Applications to the study of the molecular dynamics on cooling into the quadrupolar glass phase of solid hydrogen will be discussed.

Formation of Stimulated Echoes

A three-pulse sequence is sketched in Fig.17. As the analysis of solid echoes, the nuclear spin density matrix at different time are given by

$$\rho(0_-) = \rho_{eq} \approx \frac{1}{3}(1 + \frac{\hbar\omega_0}{KT}I_z)$$

$$\rho(0_+) = \frac{1}{3}(1 + \frac{\hbar\omega_0}{KT}I_x)$$

$$\rho(\tau_-) = e^{-\frac{i}{\hbar}\int_0^\tau H_{dd}^{sec}(t')dt'}\rho(O_+)e^{\frac{i}{\hbar}\int_0^\tau H_{dd}^{sec}(t')dt'}$$

$$\rho(\tau_+) = e^{i\psi(I_x sin\phi + I_y cos\phi)}\rho(\tau_-)e^{-i\psi(I_x sin\phi + I_y cos\phi)}$$

$$\rho[(t_w + \tau)_-] = e^{-\frac{i}{\hbar}H_{dd}^{sec}t_w}\rho(\tau_+)e^{\frac{i}{\hbar}H_{dd}^{sec}t_w}$$

$$\rho[(t_w + \tau)_+] = e^{i\psi'(I_x sin\phi' + cos\phi')}\rho[(t_w + \tau)_-]e^{-i\psi'(I_x sin\phi' cos\phi')}$$

$$\rho(t_w + \tau + t) = e^{-\frac{i}{\hbar}H_{dd}^{sec}t}\rho[(t_w + \tau)_+]e^{\frac{i}{\hbar}H_{dd}^{sec}t}$$

The signal

$$S(t_w + \tau + t) \propto Tr\{\rho(t_w + \tau + t)I_+\} \qquad (5.16)$$

The first preparatory pulse creates a transverse magnetization in the rotating frame. Under the influence of the Hamiltonian given by equation(5.15), the

evolution during the short time $\tau(\ll T_2)$ leads to the formation of nuclear spin states described by $\rho(\tau_-)$ which contains both transverse magnetization and transverse alignment. The transverse components are transferred by a second pulse $R(\psi)$ into longitudinal components corresponding to spin polarization and spin alignment. They will be stored and evolved during long waiting time t_w (chosen short compared with the longitudinal relaxation times). Therefore we can obtain a "fingerprint" of the local alignments σ. After the waiting period $t_w \ll T_2$ the stored components can now be 'read' by means of a third pulse of rotation angle ψ'. The spin polarization and spin alignment 'stored' during t_w are transferred by the third pulse into coherent transverse states, which then evolve in a reverse manner to that occurring during the first evolutionary period τ and the transverse signal focuses to stimulated echo after a delay time τ following the third pulse.

$$Tr\{\rho(t_w + \tau + t)I_+\}$$

$$= \frac{1}{3}\frac{\hbar\omega_0}{KT}\sum_{m_1-m_{12}}\langle m_1 \mid e^{-\frac{i}{\hbar}H_{dd}^{sec}t} \mid m_2\rangle\langle m_2 \mid R(\phi') \mid m_3\rangle\langle m_3 \mid e^{-\frac{i}{\hbar}H_{dd}^{sec}t_w} \mid m_4\rangle$$

$$\langle m_4 \mid R(\phi) \mid m_5\rangle\langle m_5 \mid e^{-\frac{i}{\hbar}H_{dd}^{sec}\tau} \mid m_6\rangle\langle m_6 \mid I_x \mid m_7\rangle$$

$$\langle m_7 \mid e^{\frac{i}{\hbar}H_{dd}^{sec}\tau} \mid m_8\rangle\langle m_8 \mid R(\phi) \mid m_9\rangle\langle m_9 \mid e^{\frac{i}{\hbar}H_{dd}^{sec}t_w} \mid m_{10}\rangle$$

$$\langle m_{10} \mid R^+(\phi') \mid m_{11}\rangle\langle m_{11} \mid e^{\frac{i}{\hbar}H_{dd}^{sec}t} \mid m_{12}\rangle\langle m_{12} \mid I_+ \mid m_1\rangle \qquad (5.17)$$

Since the calculation is extremely tedious and the results for general ϕ,ϕ' and general ψ,ψ' are very complicated, we only investigate the results of calculations by taking two special cases.

(1)

$$\phi = 0, \phi' = \frac{\pi}{2}$$
$$\psi = \frac{\pi}{2}, \psi' = \frac{\pi}{2}$$

This is a $90_y^\circ - \tau - 90_y^\circ - t_w - 90_x^\circ$ pulse sequence

$Tr\{\rho(t_w + \tau + t)I_+\}$

$$= \frac{3}{2}\frac{\hbar\omega_0}{KT}e^{-i\Delta\omega t}i\cos(\Delta\omega\tau)\cos^2(\Delta\omega t_w)\cos[\frac{1}{2}DP_2(\theta)\sigma(t - \tau)]$$

$$+\frac{3}{2}\frac{\hbar\omega_0}{KT}e^{-i\Delta\omega t}i\cos(\Delta\omega\tau)\sin^2(\Delta\omega t_w)\cos[\frac{1}{2}DP_2(\theta)\sigma(t + \tau)]$$

$$-\frac{2}{3}\frac{\hbar\omega_0}{KT}e^{-i\Delta\omega t}\sin(\Delta\omega\tau)\sin(\Delta\omega t_w)\cos[\frac{1}{2}DP_2(\theta)\sigma(t - t_w + \tau)] \qquad (5.18)$$

(2)

$$\phi = \frac{\pi}{2}, \phi' = \frac{\pi}{2}$$
$$\psi = \frac{\pi}{2}, \psi' = \frac{\pi}{2}$$

This is a $90_y^\circ - \tau - 90_x^\circ - t_w - 90_x^\circ$ pulse sequence

$Tr\{\rho(t_w + \tau + t)I_+\}$

$$= \frac{2}{3}\frac{\hbar\omega_0}{KT}e^{-i\Delta\omega t}i\sin^2(\Delta\omega t_w)\sin(\Delta\omega\tau)\cos[\frac{1}{2}DP_2(\theta)\sigma(t - \tau)]$$

$$+\frac{2}{3}\frac{\hbar\omega_0}{KT}e^{-i\Delta\omega t}i\sin(\Delta\omega\tau)\cos^2(\Delta\omega t_w)\cos[\frac{1}{2}DP_2(\theta)\sigma(t + \tau)]$$

$$+\frac{2}{3}\frac{\hbar\omega_0}{KT}e^{-i\Delta\omega t}\cos(\Delta\omega t)\cos(\Delta\omega t_w)\cos[\frac{1}{2}DP_2(\theta)\sigma(t - t_w + \tau)] \qquad (5.19)$$

Examining expressions of eqs.(5.18) and (5.19), besides the echo at $t = \tau$ after the third pulse, there is a additional echo at $t = t_w - \tau$. The results are sketched in Fig.18. The appearance of multipole echoes has been seen in experiments (Fig.19) for ortho-para hydrogen mixtures at low temperatures.

Engelsberg et al. (81) have presented results for nuclear spin stimulated echoes in glasses. The curve of ^{11}B echoes in borosilicate glass at 4.2 K (Fig.20) shows that in addition to the solid echo at $t = 2\tau$(after first pulse) and a stimulated echo at $t = T + 2\tau$, other echoes at $t = 2T$ (image echo) and $t = 2T + 2\tau$ (primary echo) were clearly observed. For longer waiting times, the solid echo(which they called spontaneous echo) decays rapidly and only the stimulated echo remains detectable.

Fig.21 shows the temperature dependence of the $\left(\frac{\pi}{2} - \tau - \frac{\pi}{2} - t_w - \frac{\pi}{2}\right)$ stimulated in the quadrupolar glass phase of solid hydrogen ($\tau = 25\mu s$, $t_w = 2ms$). The theoretical results (eqs 5.18 and 5.19) and the experimental results clearly show that the amplitude of stimulated echo is proportional to $\frac{1}{T}$. For experimental curve only a very slight modificaion (indicated by the arrow) was observed. We will discuss this phenomenon later.

The experimental curve in Fig.22 gives the relation of stimulated echo versus waiting time t_w of solid hydrogen (ortho-concentration $x = 0.54$, $T = 220mK$). The time scale is logarithmic. The logarithmic decay behavior can be understood in terms of the motional damping of stimulated echoes.

Low-Frequency Dynamics of Orientational Glasses

The orientational glasses (20, solid ortho-para H_2 mixtures (6), N_2/A mixtures (83) and the $KBr_{1-x}K(CN)_x$ mixed crystals (82, 84, 85)) form a subgroup of the general family of spin-glasses which continue to generate intense interest because of the apparently universal low temperature properties observed for a very diverse range of examples (dilute magnetic alloys, mixed crystals, dilute mixtures of rotors, partially doped semiconductors (86), Josephson junction arrays (87) and others). The most apparent striking universal features (20) are an apparent freezing of the local degrees of freedom on long time scales without any average periodic long range order, characteristic slow relaxations and history-dependence following external field (magnetic, electric, elastic-strain....) perturbations, and a very large number of stable low energy states.
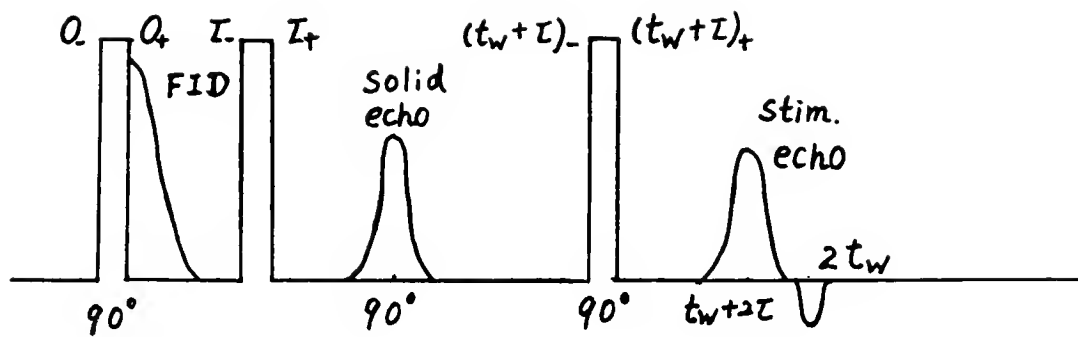
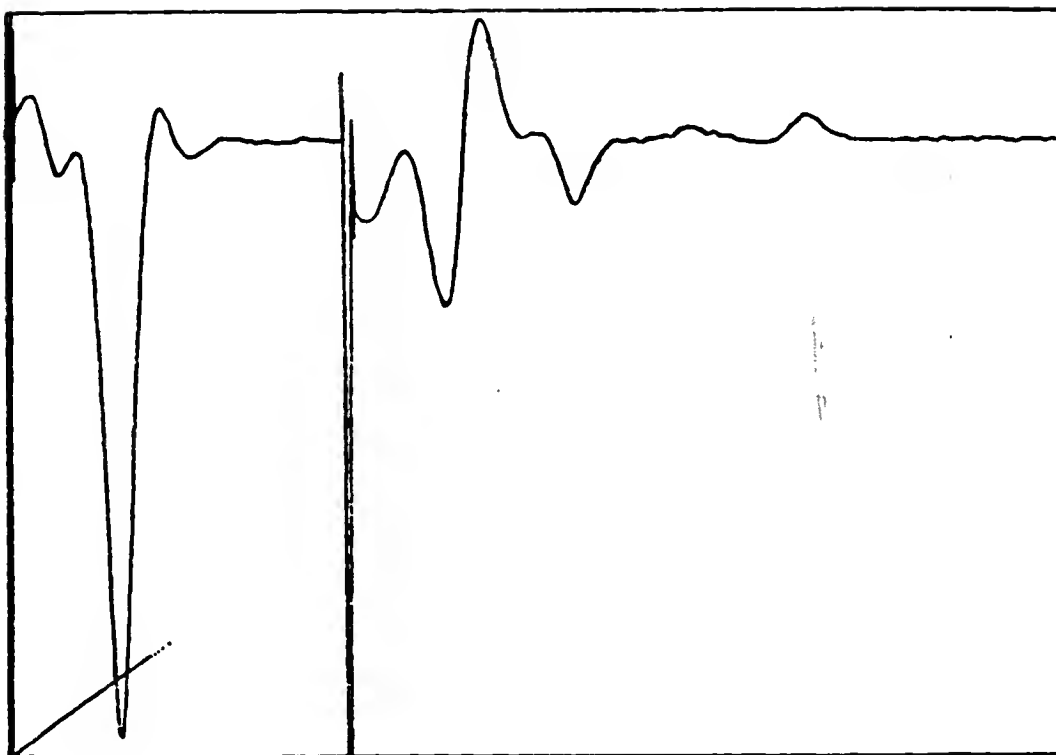Figure 18. Sketch of The Results of Calculations

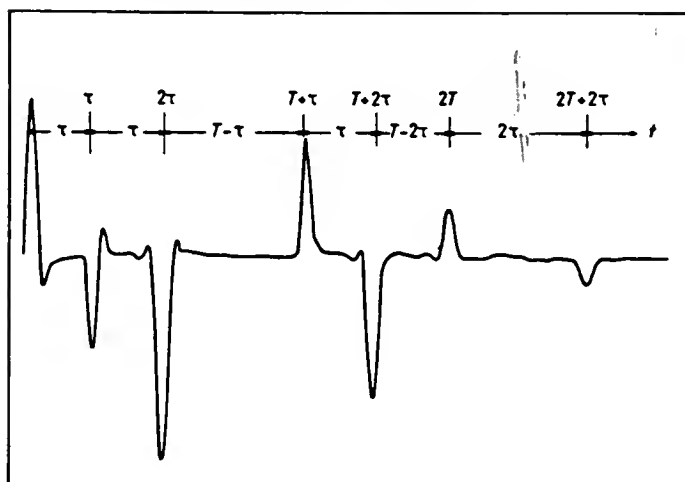Figure 19. Experimental Curve ($x = 23\%, T = 38mK$)

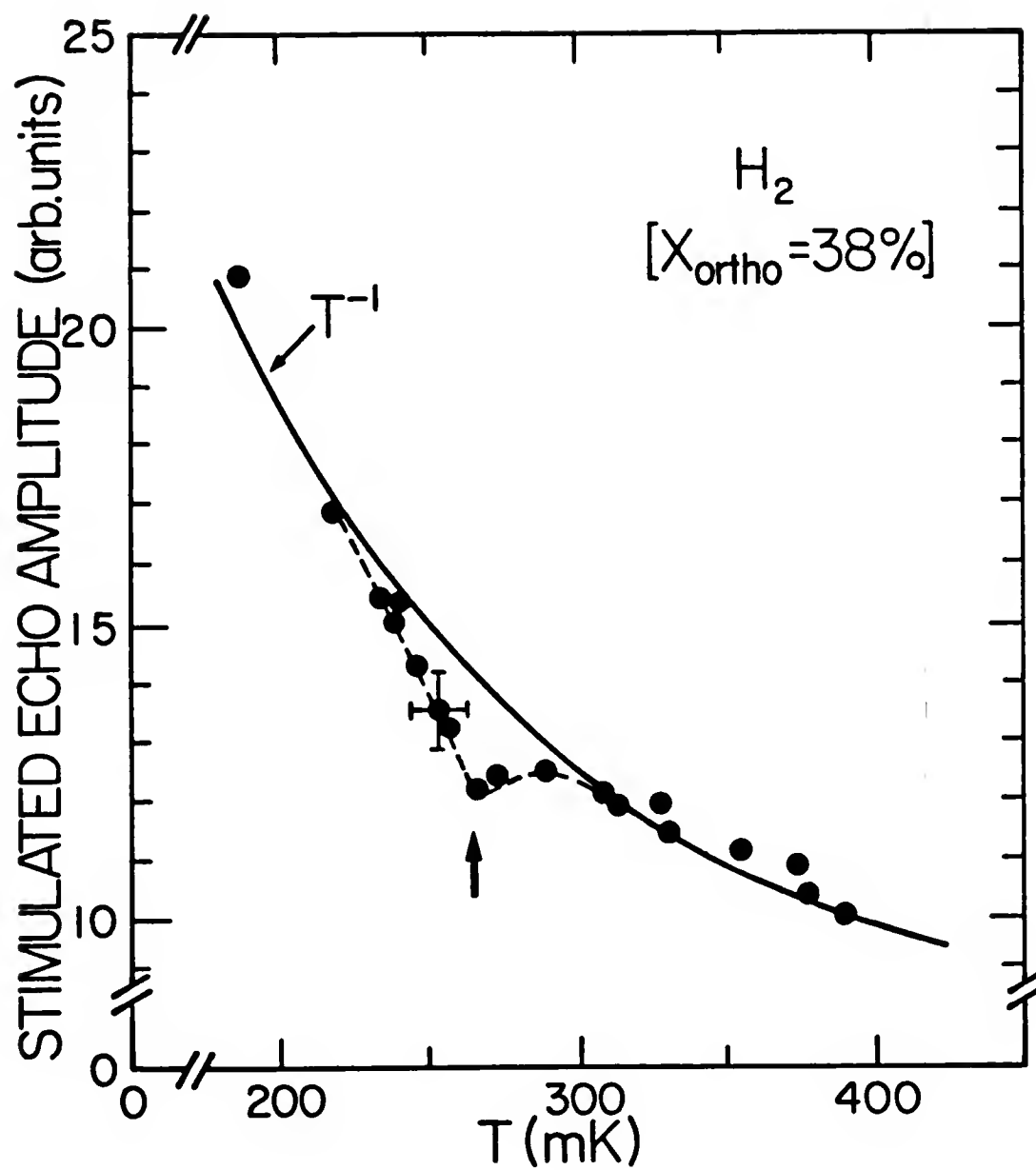Figure 20. ^{11}B Spin Echoes in Borosilicate Glass at 4.2K

Figure 21. Temperature Dependece of
$\frac{\pi}{2}-\tau-\frac{\pi}{2}-t_w-\frac{\pi}{2}$
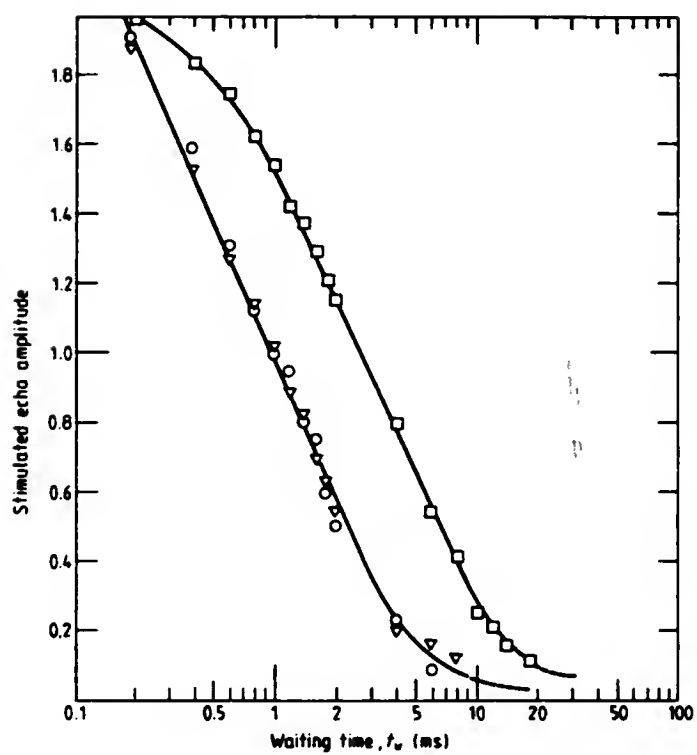Sequence ($\tau = 25\mu s, t_w = 2ms$)

Figure 22. The Observed Decay of Stimulated Echo
$(x = 0.54,\ T = 220mK)$
(squares:$\tau = 12.5\mu s$; circles and triangles:
$\tau = 25\mu s$)

The echo calculation mentioned above was based on the static case. If the ortho molecules are in slow motion, the stimulated echoes will be damped. At low temperatures the random occupation of lattice sites for solid H_2 mixtures (for $X < 55\%$) leads automatically to the existence of local electric field gradients, the field conjugate to the local order parameter, which plays the same role as the magnetic field for the dipolar spin glasses. This random local field therefore makes the problem of local orientational ordering in random mixtures equivalent to the local dipolar ordering in spin glasses in the presence of random magnetic fields.

In analogy with the analysis for spin glasses we assume that the existence of local electric field gradients leads to clusters (or droplets) of spins (88). Based on Fisher and Huse's recent picture (89), we provide a explanation of the low-frequency relaxation and the low-temperature specific heat of solid ortho- para hydrogen mixtures.

In the scaling model of Fisher and Huse the low-energy excitations which dominate the long-distance and long-time correlations are given by clusters of coherently reoriented spins. Their basic assumptions are:

(1) Density of states at zero energy for droplets (d dimension) length scale L as $L^{-\theta}$, where $0 < \theta \leq \frac{d-1}{2}$.

(2) Free energy barriers E_B for cluster formation scale as $E_B \sim L^{\psi}$ with $\theta \leq \psi \leq d - 1$.

With these assumptions, Fisher and Huse show that the autocorrelation function

$$C_i(t) = \langle \langle S_i(0)S_i(t) \rangle_t - \langle S_i \rangle_t^2 \rangle_c \qquad (5.20)$$

decays as $(\log t)^{-\frac{\theta}{\psi}}$ for $t \to \infty$.

For our system, assuming axial symmetry, the quasi-static local orientational order parameters are the alignments $\sigma_i = \langle 3J_z^2 - 2 \rangle_i$ and the corresponding autocorrelation functions $C_i(t) = \sigma_i(0)\sigma_i(t)$ can be studied directly by NMR.

For a $90°y - \tau - 90°y - t_w - 90_x^\circ$ pulse sequence we assume at $t = \tau$, order parameter $\sigma = \sigma(\tau)$ and at $t = \tau + t_w$, $\sigma = \sigma(\tau + t_w)$ for each ortho molecule

$$Tr\{\rho(t_w + \tau + t)I_+\}$$

$$= \frac{2}{3}\frac{\hbar\omega_0}{KT}e^{-i\Delta\omega t}i\cos(\Delta\omega\tau)\cos^2(\Delta\omega t_w)\cos[\frac{1}{2}DP^2(\theta)\sigma(\tau + t_w)t - \frac{1}{2}DP_2(\theta)\sigma(\tau)\tau]$$

$$+ \frac{2}{3}\frac{\hbar\omega_0}{KT}e^{-i\Delta\omega t}i\cos(\Delta\omega\tau)\sin^2(\Delta\omega t_w)\cos[\frac{1}{2}DP_2(\theta)\sigma(\tau + t_w)t + \frac{1}{2}DP_2(\theta)\sigma(\tau)\tau]$$

$$- \frac{2}{3}\frac{\hbar\omega_0}{KT}e^{-i\Delta\omega t}\sin(\Delta\omega\tau)\sin(\Delta\omega t_w)$$

$$\cos[\frac{1}{2}DP_2(\theta)\sigma(\tau + t_w)t - \frac{1}{2}DP_2(\theta)\sigma(\tau + t_w)t_w + \frac{1}{2}DP_2(\theta)\sigma(\tau)\tau] \quad (5.21)$$

Considering $t = \tau$, the stimulated echo amplitude

$$A \propto \langle\langle \cos[D_i\tau\sigma_i(\tau)]\cos[D_i\tau\sigma_i(\tau + t_w)] \rangle\rangle \quad (5.22)$$

where the double brackets refer to an average of configuration and $D_i = \frac{1}{2}DP_2(\cos\theta_i)$. The important point is that if the local order parameters σ_i remain fixed during t_w, there is no damping of the stimulated echo, while σ_i changes due to local re-orientations, then the contribution to the echo is severely attenuated. The product $D\tau$ can in practice be made very large and this method can therefore be used to study ultra-slow motions in solids. We believe that in Fig.21 the departure portion from $\frac{1}{T}$ (indicated by an arrow) is due to slow motion.

A barrier will have a characteristic life time given by an Arrhenius Law

$$\frac{1}{\Gamma} = \frac{1}{\Gamma_0}e^{\frac{E_B}{K_B T}}$$

or tunneling rate Γ

$$\Gamma(E_B) = \Gamma_0 e^{-\frac{E_B}{K_B T}} \qquad (5.23)$$

where Γ_0 is the characteristic attempt frequency for clusters of this size. In the long time limit Γ_0 is resonably well-defined because it is associated with a characteristic cluster size. In a time t the only barriers crossed will be those satisfying $0 \leq E_B \leq E_{max}(t)$ where $E_{max}(t) = K_B T \log \frac{t}{t_0}$. Any barriers crossed lead to significant changes in the local order parameters and the amplitude of the stimulated echo is then simply

$$A(t) = \int_{E_{max}(t)}^{\infty} P(E_B) dE_B \qquad (5.24)$$

At low temperatures, assuming a constant density of barrier heights $P(E_B)$, we find

$$A(t) = 1 - K_B T P_0 \log(\frac{t}{t_0}) \qquad (5.25)$$

The prefactor P_0 can be determined from the low temperature behavior of the heat capacity.

For the ortho-H_2 molecules with angular momentum $J = 1$, we can associate a simple two level system with the energy states for a given molecules; the states $J_{\varsigma_i} = \pm 1$ being separated from the state $J_{\varsigma_i} = 0$ by a gap $3\Delta_i$ (The states $J_{\varsigma_i} = \pm 1$ are degenerate if there are no interactions which break time reversal symmetry). At low energies we can, following the above arguments, identify the low energy excitations (which determine C_v at low T) with a broad quasi-constant distribution $P(\Delta)$ for $0 < \Delta < \Delta_0$ for the spins in a cluster. Identifying $P(\Delta = 0)$ with P_0, the density of low energy barriers, we have

$$\frac{C_v}{NxR} = P_0 \int_0^{\Delta_0} \frac{18}{K^2 T^2} \frac{\Delta^2}{4e^{-\frac{3\Delta}{K_B T}} + e^{\frac{3\Delta}{K_B T}} + 4} d\Delta \qquad (5.26)$$

where x is the ortho-H_2 concentration.

let $u = 3\frac{\Delta_0}{K_B T}$

$$\frac{C_v}{N x R} = P_0 \frac{2 K_B T}{3} \int_0^{3\frac{\Delta_0}{K_B T}} \frac{u^2}{4e^{-u} + e^u + 4} du \qquad (5.27)$$

set $t = \frac{K_B T}{\Delta_0}$

$$\frac{C_v}{N x R} = P_0 \Delta_0 \frac{2}{3} t \int_0^{\frac{3}{t}} \frac{u^2 du}{4e^{-u} + e^u + 4} \qquad (5.28)$$

let

$$C_v' = \frac{2}{3} t \int_0^{\frac{3}{t}} \frac{u^2 du}{4e^{-u} + e^u + 4} \qquad (5.29)$$

The resulting C_v' (Figure 23) has a linear temperature dependence at low T and a peak at $T_{pk} = 0.70\frac{\Delta_0}{K_B}$ in close resemblance to the temperature behavior observed by Haase et al. (90). From the peak position in the experimental data, $\frac{K_B}{\Delta_0} = 1.27$, $P_0 K = 0.86$ and for the stimulated echo decay this value gives

$$A_{calc.}(t) = 1 - 0.43 \log_{10}(\frac{t}{t_0}) \qquad (5.30)$$

and the observed decay

$$A_{obs.}(t) = 1 - 0.55 \log_{10}(\frac{t}{t_0}) \qquad (5.31)$$

at $T = 0.22K$ for $x = 54\%$. The agreement is remarkably good.

The experimental curves indicate $t_0 \sim 10^{-4}$s.

It should be noted that the argument relating the logarithmic decay to maximum barrier height crossed in time t can also apply (over a short time scale) to the case of orientational ordering in pure N_2 studied in reference (11,91) because one also observes a relatively large distribution of order parameters centered on $\sigma' = 0.86$ and with width 0.12 in this case. The essential point is that the time scale of the slow relaxations in the glass phase is simply related to the low temperature behavior of the heat capacity.

Another important point is that the characteristic times t_0 are much shorter than the spectral-diffusion time scale ($\sim sec$) seen by the recovery of holes burnt in the NMR lineshape. We therefore find it difficult to attribute the logarithmic decay seen in H_2 to spectral diffusion across the NMR linshape.
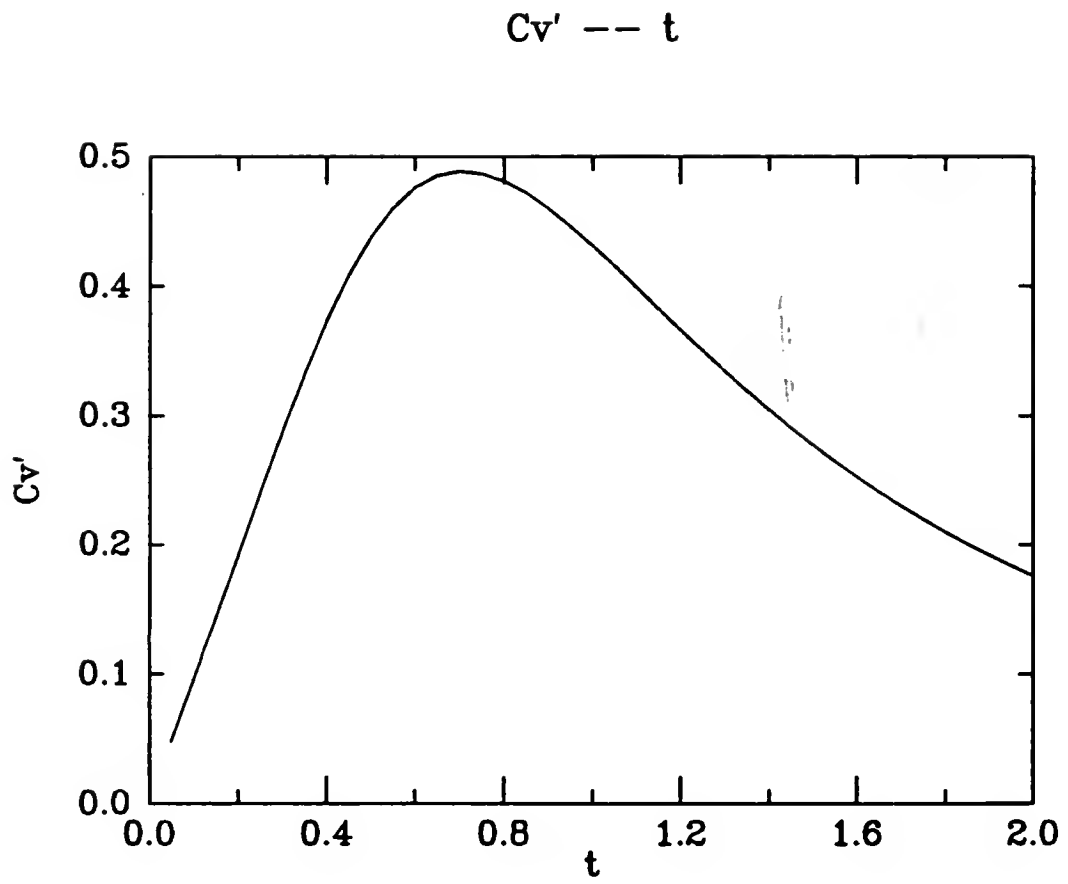
Figure 23. Calculated Curve of $C'_v - t$

CHAPTER 6

SUMMARY AND CONCLUSIONS

The ortho-para mixtures of solid H_2 are studied theoretically for fcc lattices ($X \geq 0.55$) of finite site by Akira Mishima and Hiroshi Miyagi (92). The systematic theoretical studies of nuclear magnetism for quadrupolar glass regime are carried out in this dissertation.

We have developed a theory of the nuclear spin-lattice relaxation of orientationally ordered ortho hydrogen molecules for the case of local ordering in the quadrupolar glass phase of solid hydrogen. We have investigated the temperature dependence of T_1. It shows that Gaussian Free Induction Decay is a quite good approximation. The calculations indicate a strong spectral inhomogeneity of the relaxation rate $T_1^{-1}(\Delta\nu)$ throughout the NMR absorption line. The detailed dependence is much stronger than the simple dependence $T_1^{-1}(\Delta\nu) \propto (2+\sigma)$ given by earlier estimates by A. B. Harris et al. (1). There is also a strong variation with the orientation of the local symmetry axis with respect to the external field. The variation is in agreement with that found by Hardy and Berlinsky (93) for the long-range ordered Pa_3 phase. If the cross-section relaxation between different isochromats is taken into account, the results of calculations of spectral inhomogeneity is in good agreement with the experimental results.

In addition to the spectral inhomogeneity, the relaxation is also found to be strongly nonexponential. This can be understood easily. As a result of the glassy nature of the system, there is a broad distribution of both local orientational order parameters(σ) and the orientation (α) of the local symmetry

85

axes for the molecular alignments. The existence of these distributions at low temperatures means that a given frequency $\Delta\nu$ in the spectrum comes from all the different allowed combinations of σ and α that satisfy $\Delta\nu = \frac{1}{2}DP_2(\alpha)\sigma$. The dependence of the relaxation rates on σ and P_2 then leads to a distribution of local relaxation rates for a fixed $\Delta\nu$. It is this distribution in rates that leads to the observed non-exponential behavior of $M(t)$. Calculations based on the expected probability distributions for σ and P_2 yield results in good agreement with the results reported in the publications (14).

The most important conclusion of the study of T_1 is that the spectral inhomogeneity and nonexponential recovery both results in an order of magnitude variation of the nuclear spin relaxation and must therefore be correctly understood and accounted for before attempting to analyze the experimental results in terms of the fundamental molecular motions.

We have determined that in general the orientational degrees of ortho-H_2 molecules in the solid need to be described in terms of density matrices. The ortho molecules have momentum $J = 1$ and the single particle density matrices are completely determined by five independent parameters (if the angular momentum is quenched). These parameters are

    (1) the three principal axes (x,y,z) for the second order tensor.

    (2) the alignment $\sigma' = \langle 1 - \frac{3}{2}J_Z^2 \rangle$, and

    (3) the eccentricity $\eta = \langle J_x^2 - J_y^2 \rangle$.

The positivity conditions for the density matrix show that the only allowed values of (σ', η) are those enclosed in a triangle in (σ', η) space whose vertices are the pure states $\mid J_z = 0 \rangle$ and $\mid J_z = \pm 1 \rangle$. Not all of these allowed values are physically inequivalent because one may relabel the principal axes and we have shown that one can determine a simple primitive set of order parameters

which are inequivalent by the choice $2\sigma' \geq \eta \geq 0$. Orientational states with negative σ' are not excluded on theoretical grounds.

Studies of molecular dynamics have shown the existence of para-librons, i.e. collective excitations that exist in large clusters with well-developed short range order.

Nuclear spin stimulated echoes have proved to be very effective for the study of ultra-slow molecular motions both in the molecular orientational glasses and in ordinary glasses (81). The existence of multiple echoes which is given by theoretical calculations is also in good agreement with experimental results of solid hydrogen and ordinary glass at low temperature.

We have offered a unified explanation of the slow relaxational behavior and low temperature heat capacity of the quadrupolar glass phase of solid hydrogen in terms of the density of low-energy excitations in the system.

Since the stimulated echoes are damped by any change in the orientational states during t_w, they can be used to detect very slow molecular motions. The phenomeno of logarithmic decay of the stimulated echo, which is similar to decay of magnetization in metal spin glass, can be explained by using Fisher and Huse's recent picture of the short range spin-glasses and the domination of the long-term relaxation by low energy large-scale-cluster excitations.

In analogy with spin glasses (e.g. alloys like $Cu - Mn$ where a random configuration of spins condenses at low temperature) the linear specific heat with temperature at low T can be understood in terms of the suggestion (94) that the dominant contribution to the specific heat will be from clusters of particles for which the energy barrier is sufficiently great so that resonant tunneling between the two local minima does not occur, but sufficiently small so that tunneling between the two levels can take place and thermal equilibration

can occur during the time span of the specific heat experiment. We obtained a very good linear dependence curve at low T by using a numerical integral method.

Having combined with the results of logarithmic decay of stimulated echoes and linear low-temperature specific heat, a very good numerical expression of the amplitude of the stimulated echo as a function of waiting time t_w for $x = 54\%$, $T = 0.22K$ is obtained.

Most people agree that molecular orientations of random ortho-para hydrogen mixtures become frozen at low temperature and there is no evidence for any well-defined phase transition on cooling from the completely disordered high temperature phase. However, the gradual transition to the glass state in these systems involves strong co-operativity as evidenced by Monte Carlo calculations. Studies of the nuclear relaxation and molecular dynamics have shown quantitatively how important the co-operativity is. Further theoretical study of the slow motions needs to be carried out to improve the understanding of the nature of the quadrupole ordering in random mixtures at low temperatures and their relation to the family of glasses. Further experiments at very low temperatures will also provide a deeper understanding of the properties of the quadrupolar glass state.

APPENDIX

FLUCTUATION-DISSIPATION THEOREM

The fluctuation-dissipation theorem is extremely important because it relates the response matrix to the correlation matrix for equilibrium fluctuations.

In Chapter 2 we mensioned the definitions of the response function(eq.2.32) and the relaxation function(eq.2.35). The response function my be written in a number of equivalent ways:

$$f_{kl}(t) = \frac{1}{i\hbar} Tr\{[\rho_{eq}, M_l(-t)]M_k\} \tag{A.1}$$

$$= \frac{1}{i\hbar}\langle[M_l(-t), M_k]\rangle \tag{A.2}$$

$$f_{kl}(t) = \frac{1}{i\hbar}\langle[M_l, M_k(t)]\rangle \tag{A.3}$$

Using an identity due to Kubo the response function may also be written as

$$f_{kl}(t) = \int_0^\beta ds\langle\dot{M}_l(-i\hbar s)M_k(t)\rangle \tag{A.4}$$

$$f_{kl}(t) = -\int_0^\beta ds\langle M_l(-i\hbar s)\dot{M}_k(t)\rangle \tag{A.5}$$

Here $i\hbar s$ plays the role of time. Such formulas appear in quantum statistical mechanics because of the formal similarity between the way time and temperature must be treated. In the calculation of a canonical partition function one must take into account the factor $e^{-\beta H}$. In calculating the time evolution of operators one must consider operators of the form $e^{(\frac{i}{\hbar})Ht}$. By writing $t = i\hbar s$ one can see that s will play a role identical to β in all formal developments.

From eq.(2.35) and eq.(A.5) it follows that

$$F_{kl}(t) = \int_0^\beta ds \langle M_l(-i\hbar s) M_k(t) \rangle - \lim_{T \to \infty} \int_0^\beta ds \langle M_l(-i\hbar s) M_k(T) \rangle \quad \text{(A.6)}$$

As T apparoches infinity in the second term of Eq.(A.6) we can assume that the correlation is lost between various components of the magnetization so that the correlation function factors into $\langle M_l \rangle \langle M_k \rangle$. Hence the relaxation function may be written in its more usual form

$$F_{kl}(t) = \int_0^\beta ds \langle \Delta M_l(-i\hbar s) \Delta M_k(t) \rangle \quad \text{(A.7)}$$

In this form there exists a mathematical identity between the relaxation function and the correlation function $g_{kl}(t)$, given by

$$F_{kl}(t) = \int_{-\infty}^{+\infty} B(t - \tau) g_{kl}(\tau) d\tau \quad \text{(A.8)}$$

where

$$g_{kl}(t) = \frac{1}{2} \langle [\Delta M_k(t), \Delta M_l(0)]_+ \rangle \quad \text{(A.9)}$$

the + subscript indicates the anticommutator; or in terms of Fourier transforms

$$\hat{g}_{kl}(\omega) = \frac{\hat{F}_{kl}(\omega)}{\hat{B}(\omega)} \quad \text{(A.10)}$$

where

$$B(t) = \frac{3}{\hbar \pi} \log[coth(\frac{\pi |t|}{2\beta\hbar})] \quad \text{(A.11)}$$

and

$$\frac{1}{\hat{B}(\omega)} = \frac{\hbar\omega}{2} coth \left(\frac{\beta\hbar\omega}{2} \right) \quad \text{(A.12)}$$

The derivation of these identities is called the quantum-mechanical fluctuation dissipation theorem. This theorem relates the response of step function disturbance to the correlation function of fluctuations in the equilibrium ensemble.

In the classical limit $(\hbar \to 0) B(t) \to \beta\delta(t)$, and one obtains the classical fluctuation-dissipation theorem

$$F_{kl}(t) = \beta g_{kl}(t) \quad \text{(A.13)}$$

REFERENCES

1. A. B. Harris and H. Meyer, Can. J. Phys. 63, 3 (1985)

2. N. S. Sullivan and R. V. Pound, Phys. Rev. A6, 1102 (1972)

3. N. S. Sullivan, in "Quantum Fluids and Solids" (Eds. E. D. Adams and G. G. Ihas) AIP Cof. Proc. 103, 109, AIP, New York (1983)

4. N. S. Sullivan, H. J. Vinegar and R. V. Pound, Phys. Rev. B12, 2596 (1975)

5. J. R. Gaines, A. Mukherjee and Y. C. Shi, Phys. Rev. B17, 4188 (1978)

6. N. S. Sullivan, M. Devoret, B. P. Cowan and C. Urbina, Phys. Rev. B17, 5016 (1978).

7. J. V. Gates, P. R. Ganfors, B. A. Fraas, and R. O. Simmons, Phys. Rev. B19,3667 (1979)

8. D. G. Haase, J. O. Sears and R. A. Orban, Solid State Commun. 35, 891 (1980)

9. D. Candela, S. Buchman, W. T. Vetterling and R. V. Pound, Physica$(B + C)$ 107, 187 (1981)

10. D. Candela and W. T. Vetterling, Phys. Rev. B25, 6655 (1982)

11. N. S. Sullivan, D. Esteve and M. Devoret, J. Phys. C (Solid State) 15, 4895 (1982)

12. D. Esteve, M. Devoret and N. S. Sullivan, J. Phys. C (Solid State) 15, 5455 (1982)

13. A. B. Harris, S. Washburn and H. Meyer, J. Low Temp Phys., 50, 151 (1983)

14. I. Yu, S. Washburn, M. Calkins and H. Meyer, J. Low Temp Phys., 51, 401 (1983)

15. M. A. Klenin, Phys. Rev., B28, 5199 (1983)

16. J. R. Gaines and P. Sokol, in "Quantum Fluids and Solids" (Eds. E. D. Adams and G. G. Ihas), AIP Cof. Proc., 103, 84, AIP, New York (1983)

17. D. G. Haase and M. A. Klenin, Phys. Rev. B28, 1453 (1983)

18. H. Meyer and S. Washburn, J. Low Temp. Phys., 57, 31 (1984)

19. M. Calkins and H. Meyer, J. Low Temp. Phys. 57, 265 (1984)

20. Debashish Chowdhury, "Spin Glasses and Other Frustrated Systems", Princeton Series in Physics, Princeton, New Jersey (1986)

21. H. Maletta and W. Felsch, phys. Rev. B20, 1245 (1979)

22. Y. Lin and N. S. Sullivan, Mol. Cryst. Liq. Cryst. 142, 141 (1987)

23. X. Li, H. Meyer and A. J. Berlinsky, Submitted for publication (1987)

24. N. S. Sullivan, C. M. Edwards, Y. Lin and D. Zhou, Can. J. Phys.(in press) (1987)

25. N. S. Sullivan and D. Esteve, Physica $B + C$ 107, 189 (1981)

26. D. Candela, S. Buchman, W. T. Vetterling, and R. V. Pound, Physica $B + C$ 107, 187 (1981)

27. W. T. Cochran, J. R. Gaines, R. P. McCall, P. E. Sokol, and B. Patton, Phys. Rev. Lett. 45, 1576 (1980)

28. S. Washburn, M. Calkins, H. Meyer, and A. B. Harris, J. Low Temp. Phys., 53, 585 (1983)

29. N. S. Sullivan, M. Devoret, and D. Esteve, Phys. Rev. B30, 4935 (1984)

30. Y. Lin and N. S. Sullivan, J. Low Temp. Phys. 65, 1 (1986)

31. Y. Lin , C. M. Edwards and N. S. Sullivan Phys. Letters A, 118, 309 (1986)

32. W. Lakin, Phys. Rev. 98, 139 (1955)

33. D. Zwanziger, Phys. Rev. 136, B558 (1964)

34. P. Minnaert, Phys. Rev. 151, 1306 (1966)

35. U. Fano, "Spectroscopic and Group Theoretical Methods in Physics", North Holland, Amsterdam (1968)

36. M. Devoret, thesis, Universite de Paris-Sud (1982)

37. N. S. Sullivan, M. Devoret and J. M. Vaissiere, J. de Phys. (Paris) 40, L559 (1979)

38. D. S. Metzger and J. R. Gaines, Phys. Rev. 147, 644 (1966)

39. D. Esteve and N. S. Sullivan, J. Phys. C: Solid State Phys. 15, 4881 (1982)

40. I. Yu, S. Washburn, and H. Meyer, J. Low Temp. Phys. 51, 369 (1983)

41. N. Bloembergen, E. M. Purcell, and R. V. Pound, Phys. Rev. 73, 679 (1948)

42. E. R. Andrew, "Nuclear Magnetic Resonance" Cambridge Univ. Press, Cambridge, London, New York, New Rochlle, Melbourne, Sydney (1959)

43. H. Mori, Progr. Theor. Phys., 33, 423 (1965)

44. J. T. Hynes and J. M. Deutch, in "Mathematical Methods" (Eds. H. Eyring, W. Jost, and D. Henderson) Academic Press, Physical Chemistry, Vol. 11, New York (1974)

45. Daniel Kivelson and Kenneth Ogan, Adv. Mag. Res. 3, 71 (1968)

46. L. E. Reichl, "A Modern Course in Statistical Physics", University of Texas Press, Austin (1980)

47. R. Kubo and K. Tomita, J. Phys. Soc. Jap., 9, 888 (1954)

48. R. Kubo, J. Phys. Soc. Jap. 12, 570 (1957)

49. J. M. Deutch and Irwin Oppenheim, Adv. Mag, Res. 3, 43 (1968)

50. A. G. Redfield, Adv. Mag. Res. 1, 1 (1965)

51. A. Abragam, "The Principles of Nuclear Magnetism", Oxford Univ. Press, London and New York (1961)

52. C. P. Slichter, "Principles of Magnetic Resonance", Springer-Verlag, Berlin, Heidelberg, New York (1980)

53. I. F. Silvera, Rev. Mod. Phys. 52, 393 (1980)

54. A. B. Harris and L. I. Amstutz, H. Meyer, and S. M. Myers, Phys. Rev. 175, 603 (1968)

55. A. B. Harris, Phys. Rev. B1, 1881 (1970)

56. A. B. Harris, Phys. Rev. B2, 3495 (1970)

57. H. Ishimoto, K. Nagamine and Y. Kimura, J. Phys. Soc. Jap. 35, 300 (1973)

58. V. A. Slusarev and Yu. A. Freiman, J. Low Temp. Phys. 9, 97 (1972)

59. H. Ishimoto, K. Nagamine, Y. Kimura and H. Kumagai, J. Phys. Soc. Jap. 40, 312 (1976)

60. Yan-Chi Shi, J. R. Gaines an A. Mukherjee, Phys. Letters 63A, 342 (1977)

61. F. Weinhaus and H. Meyer, Phys. Rev. B7, 2974 (1973)

62. L. I. Amstutz, H. Meyer, S. M. Meyers, and R. L. Mills, J. Phys. Chem. Solids 30, 2693 (1969)

63. C. W. Myles and C. Ebher, Phys. Rev. B11, 2339 (1975)

64. C. C. Sung, Phys. Rev. 167, 271 (1968)

65. J. Hama, T. Inuzuka, and T. Nakamura, Prog. Theor. Phys. 48, 1769 (1972)

66. C. Ebner and C. C. Sung, Phys. Rev. B8, 5226 (1973)

67. C. Ebner and C. W. Myles, Phys. Rev. B12, 1638 (1975)

68. C. C. Sung and L. G. Arnold, Phys. Rev. B7, 2095 (1973)

69. M. Blume and J. Habbard, Phys. Rev. B1, 3815 (1970)

70. Sean Washburn, Insuk Yu and Host Meyer, Phys. Letters 85 A, 365 (1981)

71. W. Kinzel and K. H. Fischer, Solid State Commun., 23, 687 (1977)

72. Y. Lin and N. S. Sullivan, in "Proc. XVIII th Int. Conf. on Low temperature Physics", Elsevier Sci. Publ. EL2, 1005 (1984)

73. Karl Blum, "Density Matrix Theory and Applications", Plenum Press, New York and London (1981)

74. J. H. Van Vleck, "The Theory of Electric and Magnetic Susceptibilities", Oxford University Press, London, New York, 287 (1932)

75. Jan Van Kranendonk, "Solid Hydrogen", Plenum Press, New York, London (1983)

76. F. Reif and E. M. Purcell, Phys. Rev. 91, 63 (1953)

77. C. M. Edwards, D. Zhou and N. S. Sullivan, Phys. Rev. B34, 6540 (1986)

78. Myron G, Semack, James E, Kohl, David White, and J. R. Gaines, Phys. Rev. B18, 6014 (1978)

79. J. A. Tjon, physica 108A, 27 (1981)

80. J. E. Tanner, The Journal of Chemical Physics, 52, 2523 (1970)

81. M. Engelsberg and Nilson Mendes Borges, J. Phys. C: Solid State Phys. 17, 3633 (1984)

82. A. Loidl and K. Knorr, in "Dynamic Aspects of Structural Change in Liquid and Glasses" (Eds. C. Austen Angell and Martin Goldstein), Annals, N. Y. Acad. Sci., 484, 121, New York (1986)

83. D. Esteve and N. S. Sullivan, J. de. Phys. Lett. (Paris) 43, L793 (1982)

84. J. J. De Yoreo, M. Meissner, R. O. Pohl, J. M. Rowe, J. J. Rush and S. Susman, Phys. Rev. Lett. 51, 1050 (1983)

85. M. Meissner, W. Kneak, J. P. Sethna, K. S. Chow, J. J. De Yoreo and R. O. Pohl, Phys. Rev. B32, 6091 (1985)

86. M. Gruenewald, B. Pohlmann, L. Schweitzer and D. Wuertz, J. Phys. C15, L1153 (1982)

87. C. Ebner and D. Stroud, Phys. Rev. B31, 165(1985); S. John and T. C. Lubensky, Phys. Rev. Lett. 55, 1014 (1985)

88. M. Cyrot, Solid State Communications, 39, 1009 (1981)

89. Daniel S. Fisher and David A. Huse, Phys. Rev. Lett. 56, 1601 (1986)

90. D. G. Haase, L. R. Perrell and A. M. Saleh, J. Low Temp. Phys. 55, 283 (1984)

91. L. G. Ward, A. M. Saleh and D. G. Haase, Phys. Rev. B27, 1832 (1983)

92. Akira Mishima and Hiroshi Miyagi, J. Phys. Soc. Jap., 55, 3618 (1986)

93. W. N. Hardy and A. J. Berlinsky, Phys. Rev. B8, 4996 (1973)

94. P. W. Anderrson, B. I. Halperin and C. M. Varma, A Journal of Theoretical, Experimental and Applied Physics, eighth series- Vol. 25, 1 (1971)

BIOGRAPHICAL SKETCH

Ying Lin was born in China, on June 9, 1946. She was educated in several cities in China. She entered the department of physics at The University of Science and Technology of China as a undergraduate student in 1962 and was awarded a B.S in 1968(because the "cultural revolution," graduation was delayed).
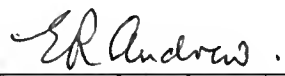
During 1968-1978 she worked in a factory (First Tractor Manufactory) and at a institute (Chinese Electronic Engineering Design Institute) as an engineer. After the "cultural revolution" she made up her mind to study physics again. She passed the entrance exam and became a graduate student in The General Research Institute for Nonferrous Metals in Peking in 1979. She obtained an M.S. of Engineering in 1981. After that she decided to go to the United States for further studies.

In September of 1981 she came to the United States. Since September of 1981 she has been a graduate student in the Department of Physics at the University of Florida. She began research under Professor Neil S. Sullivan at the end of 1983 and worked on the NMR theory of solid hydrogen at low temperatures.
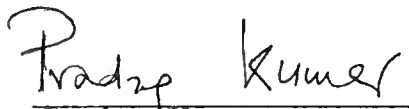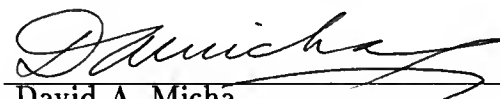
I certify that I have read this study and that in my opinion it conforms to acceptable standards of scholarly presentation and is fully adequate, in scope and quality, as a dissertation for the degree of Doctor of Philosophy.

Neil Samuel Charles Sullivan, Chairman
Professor of Physics

I certify that I have read this study and that in my opinion it conforms to acceptable standards of scholarly presentation and is fully adequate, in scope and quality, as a dissertation for the degree of Doctor of Philosophy.

E. Raymond Andew
Graduate Research Professor of Physics

I certify that I have read this study and that in my opinion it conforms to acceptable standards of scholarly presentation and is fully adequate, in scope and quality, as a dissertation for the degree of Doctor of Philosophy.

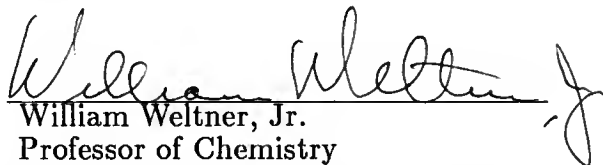Pradeep Kumar
Associate Professor of Physics

I certify that I have read this study and that in my opinion it conforms to acceptable standards of scholarly presentation and is fully adequate, in scope and quality, as a dissertation for the degree of Doctor of Philosophy.

David A. Micha
Professor of Physics

I certify that I have read this study and that in my opinion it conforms to acceptable standards of scholarly presentation and is fully adequate, in scope and quality, as a dissertation for the degree of Doctor of Philosophy.

David B. Tanner
Professor of Physics

I certify that I have read this study and that in my opinion it conforms to acceptable standards of scholarly presentation and is fully adequate, in scope and quality, as a dissertation for the degree of Doctor of Philosophy.

William Weltner, Jr.
Professor of Chemistry

This dissertation was submitted to the Graduate Faculty of the Department of Physics in the College of Liberal Arts and Sciences and to the Graduate School and was accepted as partial fulfillment of the requirements for the degree of Doctor of Philosophy.

April 1988

Dean, Graduate School

98